Progress in Oceanography 224 (2024) 103268

Contents lists available at ScienceDirect

Progress in Oceanography

journal homepage: www.elsevier.com/locate/pocean

The impact of advection on a Subarctic fjord food web dominated by the copepod *Calanus finmarchicus*

S.L. Basedow [a,*], A.H.H. Renner [b], B. Espinasse [a], S. Falk-Petersen [c], M. Graeve [d], K. Bandara [c], K. Sørensen [e], K. Eiane [f], W. Hagen [g]

[a] *UiT The Arctic University of Norway, 9037 Tromsø, Norway*
[b] *Institute of Marine Research, Fram Centre, 9296 Tromsø, Norway*
[c] *Akvaplan-niva, Fram Centre, 9296 Tromsø, Norway*
[d] *Alfred Wegener Institute, Helmholtz Centre for Polar and Marine Science, 27570 Bremerhaven, Germany*
[e] *Norwegian Institute for Water Research, Økernveien 94, 0579 Oslo, Norway*
[f] *Nord University, Faculty of Bioscience and Aquaculture, 8049 Bodø, Norway*
[g] *University of Bremen, BreMarE, Marine Zoology, 28359 Bremen, Germany*

ARTICLE INFO

Keywords:
Advection
Fjord ecosystem
Shelf ecosystem
Trophic structure
Zooplankton

ABSTRACT

Fjord and shelf food webs are frequently supplemented by the advection of external biomass, which in high-latitude seas often comes in the form of lipid-rich copepods that can support a wide range of fish species, including Northeast Arctic cod (*Gadus morhua*). A seasonal match or mismatch at the lower trophic levels (phytoplankton and zooplankton) is central in determining how much energy and biomass is available for higher trophic levels (fish). Here, we quantify the inflow of the copepod *Calanus finmarchicus* into the Vestfjorden fjord system using high-resolution measurements of ocean currents and zooplankton (laser optical plankton counter). We evaluate a spatio-temporal match/mismatch between the phytoplankton bloom and *Calanus* and assess the input of advected copeods at the lower trophic level fjord and shelf food web based on an integrative approach employing stable isotope analyses (C, N), fatty acid trophic marker analyses, and biovolume spectrum analyses. Our results suggest two different sources of the *Calanus* population in the fjord/shelf system: one fraction overwintered locally and started ascending early to feed on the phytoplankton bloom that peaked around April 11. The other fraction had only recently (end of April) been and still was being advected from the oceanic overwintering habitats. Ca. 119 g C/s of *Calanus* were advected into the fjord, comparable to the biomass of *Calanus* advected into an Arctic fjord, and the mesozooplankton community was dominated by the copepod. The fjord food web was tightly coupled between the phytoplankton spring bloom, the local part of the *Calanus* population (trophic level 1.8–2.4) and cod larvae (high levels of wax esters). On the shelf, our results suggest that the impact of advected *Calanus* in the food web is at its starting point (low trophic level, large difference of $\delta^{13}C$ of POM and *Calanus*). We highlight important factors that can contribute to the successful spawning of Northeast Arctic cod: an extended phytoplankton bloom that can support both locally and advected *Calanus*, which in turn can supply the essential nauplii prey for first-feeding cod larvae.

1. Introduction

Fjord systems are attractive spawning and nursery grounds for a wide range of fish species (Bustos et al., 2007, Seitz et al., 2014), including many of ecological and economical importance (Bustos et al., 2008, Höffle et al., 2014). In open fjords and shelf systems, advection of zooplankton is important in structuring the ecosystems, by supplying oceanic biomass and species to coastal communities (Skreslet et al., 2000; Basedow et al., 2004, Willis et al., 2006, Trudnowska et al., 2020). This surplus of potential food for developing fish larvae is one factor that might explain why these systems are attractive spawning grounds (Espinasse et al., 2016a). At the same time, the pronounced density front between coastal and oceanic water masses offshore can inhibit exchange across that front, thus creating an environment in which larvae and their planktonic food overlap in space and time (Dong et al., 2021). Food webs in shelf seas are frequently supplemented by advection of external

* Corresponding author.
E-mail address: sunnje.basedow@uit.no (S.L. Basedow).

https://doi.org/10.1016/j.pocean.2024.103268

Available online 4 May 2024

biomass, which in high-latitude seas often comes in the form of lipid-rich copepods that can support higher trophic levels when local production is low (Falk-Petersen et al., 1990, Norkko et al., 2007, Forest et al., 2011, Kitamura et al., 2017, Basedow et al., 2018, Geoffroy et al., 2019).

Some of the world's largest fish stocks are found in Subarctic shelf seas, this includes the northernmost population of Atlantic cod, the Northeast Arctic cod (*Gadus morhua*). Its main spawning location is the fjord/shelf ecosystem around the Lofoten archipelago in northern Norway (Ottersen et al., 2014). A match of first-feeding stages of cod larvae (predator) with high abundances of their main prey, nauplii of the copepod *Calanus finmarchicus*, can partly explain the recruitment success of cod (Hjort, 1926, Cushing, 1990). This so-called match/mismatch hypothesis has received considerable ecological interest (Fortier et al., 1995, Durant et al., 2007). Recent modelling analyses indicate that cod eggs released in the spawning locations around the Lofoten archipelago during the main spawning period around 1st April indeed offer the best growth conditions for developing larvae, by allowing them to grow in concert with their copepod prey (Vikebø et al., 2021), thus supporting field studies from the North Atlantic (Heath & Lough, 2007). A statistical analysis of spatio-temporal overlap between cod larvae and *C. finmarchicus* in the northern Norwegian and Barents Sea also supports the match/mismatch hypothesis, however, a spatio-temporal match of predator and prey only explained 29 % of the variance in the large-scale data (Ferreira et al., 2020). The rather small part of the variance explained might be partly due to a low spatio-temporal resolution in the available data sets, and partly due to fish larvae including phytoplankton and microzooplankton in their diet (Klungsøyr et al., 1989, Pepin & Dower, 2007).

Despite the importance of *Calanus* prey for one of the major fish stocks of the North Atlantic, surprisingly little research has investigated distribution patterns of this copepod in their main spawning location, Vestfjorden and the adjacent shelf (Ellertsen et al., 1987, Skreslet, 1989). For example, only recently overwintering copepods were observed within Vestfjorden (Espinasse et al., 2016b). The main overwintering locations of *C. finmarchicus* are the deep basins of the North Atlantic (Heath et al., 2004), including the oceanic basin off the Lofoten archipelago (Edvardsen et al., 2006). Here, interannual variability in abundance is driven mostly by lagged effects of large-scale climatic changes upstream (Weidberg and Basedow, 2019). Throughout the winter, diapausing copepods at depth in the Lofoten basin can be transported eastward in eddies embedded in the prevailing mean current, thus accumulating at the shelf break (Gaardsted et al., 2011, Dong et al., 2022). How these copepods then expand onto the shelf is not entirely clear, but Ekman transport of ascending copepods in spring might play an important role, as has been observed in ocean-shelf exchange processes of overwintering copepods in the Subarctic North Pacific (Coyle et al., 2013). In addition, deep channels and straits connecting oceanic areas directly with the shelf and with the fjord system inshore may be important for the transport of copepods onto the shelf and into Vestfjorden (Børve et al., 2021). A significant part of the *Calanus* population observed in Vestfjorden is also thought to originate from the South and entering Vestfjorden with prevailing currents along the southeastern shore (Furnes & Sundby, 1981, Espinasse et al., 2016a). However, observations to substantiate these indications are lacking and additional field data are needed to more accurately assess the contribution of different sources that contribute to *C. finmarchicus* abundance in the fjord.

At a lower trophic level, a spatio-temporal match of phytoplankton and spawning *Calanus* is required to yield sufficient densities of the essential nauplii prey for first-feeding cod larvae. How the food web is structured at the lower trophic levels (i.e. from phytoplankton to fish), significantly influences how much energy and biomass is available for higher trophic levels (Pedersen, 2022). Feeding strategies of zooplankton and fish larvae are central in this respect (Heneghan et al., 2016). For instance, cod larvae can switch from exclusively feeding on *Calanus* nauplii to including phytoplankton in their diet, indicated by green guts and confirmed by fatty acid trophic marker analyses (Klungsøyr et al., 1989). Herbivorous feeding of cod larvae has been observed at the initial feeding stage and might be especially important if nauplii abundance is low during this period (mismatch scenario). The timing and duration of the phytoplankton bloom in Vestfjorden is thus important for a match/mismatch with the developing *Calanus* cohort but can also bridge nauplii shortage during the most vulnerable life cycle stage of cod larvae.

A significant advective input of *C. finmarchicus* into the fjord/shelf ecosystem will influence the food web structure and can supplement higher trophic levels. We aim to (1) quantify the inflow of *C. finmarchicus* into Vestfjorden during the period of cod larvae growth at the end of April based on field data with high spatial resolution, and to (2) assess the *Calanus* input at the lower trophic level food web in the fjord based on an integrative approach employing stable isotope analyses (C, N), fatty acid trophic marker analyses, and biovolume spectrum theories to analyse trophic links at the base of the marine food web. Further, we aim to (3) compare the lower trophic level food web within the fjord with the one on the adjacent shelf. Finally, we will (4) evaluate a match/mismatch between *Calanus* and the primary production in the fjord by pinpointing the timing of the phytoplankton bloom based on a 10-year FerryBox time series crossing the fjord.

2. Material and methods

Vestfjorden is a large (1334 km^3 volume, 6153 km^2 surface area; Fig. S1), open (16.4 km^2 opening, S1) fjord situated just north of the polar circle (Fig. 1). Field sampling was performed with R/V "Helmer Hanssen" from 19 to 26 April 2015 and included mapping the distribution of zooplankton and water masses with high spatial resolution along five transects crossing the fjord (S1-S5), and two transects on the adjacent shelf (S7, S8), (Fig. 1, Table S1). Water velocities were measured along the same transects and were used to calculate the flux across transects. In addition to these high-resolution data sets, we sampled the zooplankton community at eight stations in the fjord (P1-P8) and three stations on the shelf (B1-B3). At these stations we also collected samples for stable isotopes and fatty acid composition, as well as data for biovolume spectrum analyses. Wind data were retrieved from the ship's weather stations for the dates April 18–25.

2.1. Transect sampling

Along the transects, data on hydrography and plankton were collected by a free-fall Moving Vessel Profiler (MVP, ODIM Brooke Ocean, Rolls Royce Canada Ltd., Herman et al., 1998) that was equipped with Conductivity-Temperature-Depth sensors (CTD; Applied Microsystems Ltd.), a fluorescence sensor (WET Labs FLRT chlorophyll *a* fluorometer) and a Laser Optical Plankton Counter (LOPC; currently no longer produced, Herman et al., 2004). The MVP is an advanced winch that allows to collect free-fall profiles while the ship moves along the transects (Ohman et al., 2012, Basedow et al., 2018). Sampling depth was from 10 m above bottom to surface, and the ship moved with 6 to 7 knots (3 – 3.6 m s^{-1}), resulting in a distance of ca. 500 m between profiles. Only data from downward profiles were used for further analyses, because in upward profiles irregularities in the flow through the instrument impair abundance estimates. Velocities of ocean currents were measured along the transects using a ship-mounted Acoustic Doppler Current Profiler (ADCP, RD Instruments Ocean Surveyor 75 kHz).

2.2. Station sampling

At the 11 stations, data on the physical environment were sampled by vertical deployment of the ship's CTD (SBE CTD; SBE911plus, Sea-Bird Scientific, U. S.). The zooplankton community was sampled by vertically stratified net hauls (WP2 with closing mechanism, 0.255 m^2

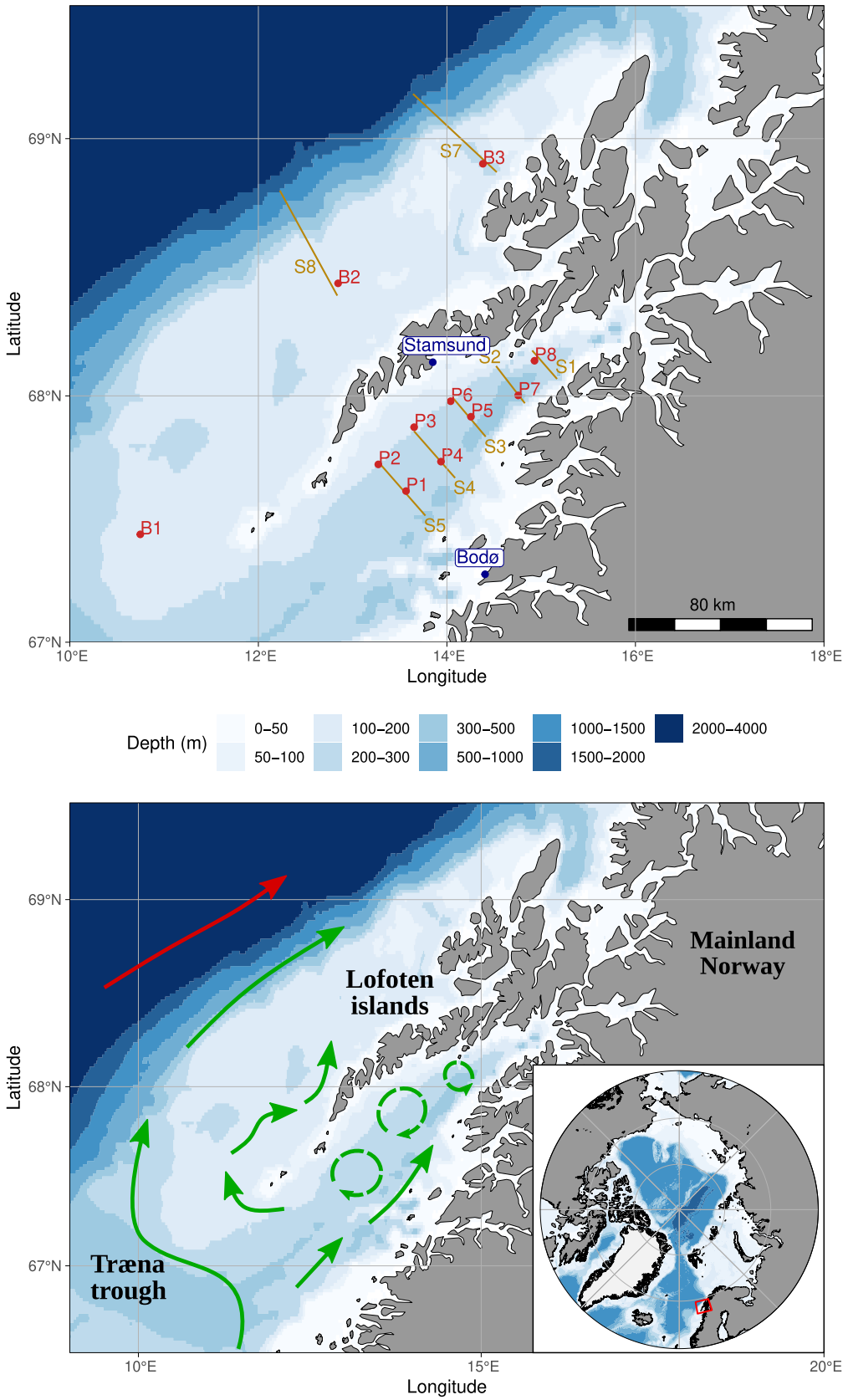

Fig. 1. Map of the study area. Top: sampling was carried out along seven transects (yellow lines) in Vestfjorden (S1 to S5) and on the shelf (S7 and S8), and at eleven stations (red dots) in Vestfjorden (P1 to P8) and on the shelf (B1 to B3). The coastal steamer "Hurtigruten" crosses the fjord from Bodø to Stamsund and is equipped with a FerryBox sampling fluorescence data. Bottom: prevailing currents, Norwegian Coastal Current (NCC) in green and the Norwegian Atlantic Current (NAC) in red.

mouth opening) using two different mesh sizes (55 and 180 μm). At most stations the depth layers 100–30-0 m were sampled by the 180 μm net, deeper layers were sampled if the station was deep enough and if time allowed for it (Table S1). *Calanus* nauplii (55 μm net) were sampled from the upper 30 m at P1, P3, P5 and P7 inside the fjord and at all three stations (B1-B3) on the shelf (Table S1). Samples were preserved in a solution of 80 % seawater and 20 % fixation agent (one part 40 % formaldehyde buffered with one part potassium bromide), resulting in a final formaldehyde concentration of 4 %). Zooplankton and ichthyoplankton specimens were also collected by a bongo net (200 and 500 μm mesh size) that was towed in the upper 30 m (matching sampling for nauplii) for 10 min at the stations inside Vestfjorden. Few fish larvae and eggs were captured in Vestfjorden, therefore, to allow for maximum capture, the bongo net was towed from bottom to surface at the shelf stations. Live *Calanus* spp. copepods and fish larvae were picked from the bongo nets and frozen at −80 °C for later analyses of lipids and stable isotopes ashore. During transport samples were stored at −20 °C for a few days. To substantiate stable isotope analyses, during the preceding winter, four *Calanus* spp. samples were collected along the continental slope off the Lofoten archipelago, and two inside Vestfjorden, stations not shown.

For the analyses of trophic flow based on biovolume spectrum theories, five to six vertical profiles of LOPC data were collected by operating the MVP in 'constant rpm' mode with the ship moving at low speed (1 knot, ca. 0.5 m s^{-1}), Table S1. Additional oceanographic measurements and water samples were collected at the stations by using the ship's Seabird Electronics 911 + CTD attached to a rosette-sampler with twelve 5L Niskin bottles. 50–100 mL seawater was collected from five depths in the upper 100 m, for analyses of chlorophyll *a* (chl *a*). Salinity samples for calibration of the conductivity cell were taken at selected stations and depths. These were analysed after the cruise at UiT using a Guildline Portasal salinometer. Additionally, at the shelf stations ca. 5 L seawater were collected from the Niskin bottles and filtered through a GF/F filter for stable isotope analyses of particulate organic matter.

2.3. Initial data analyses

2.3.1. CTD data processing

The data from the ship's SBE CTD were processed using SBE processing software and a set of Matlab scripts to derive vertical profiles of practical salinity and *in situ* temperature at 1 db resolution. The salinity data were corrected against the salinities derived from the water samples using a constant offset for the entire dataset. The MVP-CTD data were then cross-calibrated against the ship-CTD by using MVP profiles taken immediately before or after a ship-CTD cast. Offset between MVP- and ship-CTD was estimated for both temperature and salinity using measurements in the bottom 50 m, where variability was minimal compared to the upper part of the water column.

2.3.2. ADCP data processing

The raw ADCP data were processed using a suite of Matlab routines to derive 10 min-averaged current velocities along the ship track. The barotropic components of the tidal currents were estimated using output from the NorKyst800 model (Albretsen et al., 2011) and subtracted from the ADCP-measured currents for cross-transect flux estimates. The resulting detided velocities were then linearly interpolated onto the MVP data grid.

2.3.3. Analyses related to the phytoplankton bloom

Water samples for nutrient analyses were collected during a different cruise a few days before our cruise, at three stations, sampling five depths in the upper 50 m, and one depth close to the bottom (Table S1). Triplicate subsamples of each water sample were frozen on board and analysed in the laboratory after the cruise by standard seawater methods using a Flow Solution IV analyser (O. I. Analytical, USA). Prior to the analyses, the analyser was calibrated using reference seawater from Ocean Scientific International Ltd. UK. Long-term data on the bloom development in Vestfjorden were analysed based on a 10-year time-series of fluorescence data collected by a FerryBox (Petersen et al., 2006, Sørensen et al., 2008) that is mounted on the coastal steamer "Hurtigruten", which crosses the fjord between Bodø and Stamsund (Fig. 1). Only the night data (19:30–06:00 UTC) were used to remove most of the effects of the diurnal variation in the chl *a* fluorescence.

For the stations inside Vestfjorden, water samples were collected from five depths in the upper 100 m using the rosette sampler, they were filtered on board (triplicates of 50 to 100 mL, GF/F filters, Whatman Inc., USA), and kept frozen at −80 °C until analysis ashore a few weeks after the cruise. In the laboratory ashore, chl *a* concentration was determined fluorometrically (10-AU fluorometer, Turner Designs, USA) from pigment extracts in methanol obtained from filtered seawater samples USA). For stations on the shelf, chl *a* concentrations were derived from a regression of the fluorescence sensor mounted on the MVP against filtered chl *a* values, based on the data from stations P1 to P7.

2.3.4. Zooplankton analyses

The abundance of all *Calanus* developmental stages, incl. nauplii, was quantified based on sub-samples of the 180 μm and 55 μm fixed zooplankton samples, respectively. Nauplii were not sampled at all stations (section 2.2; Table S1). At least 100 nauplii and 200 older stages were identified and enumerated under a stereo-microscope. The Calanus stage index was calculated as the abundance-weighted mean stage, assigning copepodite stages and adults values from 1 (CI) to 6 (adult females and males) as in Skjoldal et al. (2021). Although *C. finmarchicus* is by far the dominating *Calanus* species in Atlantic Water, genetic analyses have revealed the occurrence of the closely related *C. glacialis* (8–12 % of *Calanus* spp. in Vestfjorden, 0 % on the shelf) and even small *C. hyperboreus* copepodites that could not be distinguished morphologically (Choquet et al., 2017). No genetic samples were obtained during our cruise in 2015, and our data may include a few *C. glacialis* and/or *C. hyperboreus* but these will not significantly influence our analyses. Ichthyoplankton was enumerated from the 180 μm net samples, all eggs and larvae were counted. In addition, at stations P4, P6 and P7, abundance of the entire zooplankton community in the 180 μm samples was analysed under the stereo-microscope. These samples indicated an overwhelming dominance of *Calanus* in the system (section 3.4). In this paper we use the term *Calanus* referring to a community clearly dominated by *C. finmarchicus*.

In addition to the abundance estimates based on net samples collected at the stations, the distribution of older stages (CIV to adults) of *Calanus* inside Vestfjorden was analysed with high spatial resolution based on LOPC data collected along the transects. The LOPC is an automatic plankton counter that counts and measures particles passing through its sampling channel, while it is being towed through the water (Herman et al., 2004). For *C. finmarchicus* in our study area, the LOPC had previously been calibrated against net samples and against data from a video plankton recorder (Gaardsted et al., 2010; Basedow et al., 2013). We applied the analytical steps and quality checks in those studies to extract particles with characteristics of CIV copepodites to adults (hereafter, older stages) of *Calanus* from the LOPC data. Quality of the LOPC data was good with lower numbers of faulty counts (Table S2). The LOPC data were also used to construct biovolume spectra for analyses of trophic indices (section 2.5.1).

2.4. Quantifying the inflow of c. Finmarchicus into Vestfjorden

As a first step to assess the influence of different water masses in Vestfjorden on the distribution of *Calanus*, we constructed histograms of the abundance of CIV, CV and adults for the upper, freshwater-influenced layer ($S \leq 34.1$) and the lower, Atlantic Water-influenced layer ($S > 34.8$) based on LOPC data. No pronounced pycnocline was observed inside the fjord, therefore those water mass limits were chosen

based on temperature gradients and salinity (section 3.1). These two water masses reflect biologically different habitats and are of particular interest because they can point to a local or advected origin of *Calanus* in Vestfjorden. Abundance data in each of those water masses were grouped into 20 equally-spaced histogram bins between 0 and 7000 individuals m^{-3}, which was the maximum abundance along most transects. Furthermore, abundance was weighted by the maximum abundance in each water mass, and histograms were then normalized, so that the area under the histogram equaled 1.

To calculate the flux across transects, the LOPC data on abundances (ind. m^{-3}) of older stages of *C. finmarchicus* were averaged along a uniform grid consisting of 480 equally-spaced cells along the longitudinal axis, and 80 equally spaced grid cells along the depth axis. Calculations were performed using the functions meshgrid and griddata contained in python packages numpy and scipy-interpolate, respectively. Water velocities across the grid cells (m/s) were computed based on 10 min-averaged and detided values. Flux of copepods (ind. $m^{-2}\ s^{-1}$) was then computed by multiplying abundance with across-transect current for each grid cell.

2.5. Trophic flow analyses

Three complementary methods were used to characterize trophic links between *Calanus* and cod larvae and to evaluate energy flow at these lower trophic levels.

2.5.1. Biovolume spectrum analyses

The biovolume spectrum is shaped by fluxes of energy and biomass through the pelagic system (Platt & Denman, 1978, Zhou & Huntley, 1997). Accordingly, from the shape of the spectrum one can infer energy fluxes such as growth and trophic position (Zhou, 2006, Basedow et al., 2010, Giering et al., 2018). For example, growth of planktonic organisms will be visible in the spectra as a shift towards the right, while increased connectance within the pelagic community will flatten the slope. Biovolume spectra were constructed based on data collected by the LOPC along vertical profiles at seven stations in Vestfjorden (P1 to P7), and two stations on the shelf (B2 to B3); no vertical profiles were obtained at the other stations. We followed the analytical procedures described in Basedow et al. (2016), and computed biovolume spectra according to their equation 1. Based on the spectra, trophic levels of the plankton community were computed as follows,

$$\text{trophic level} = -(1 + \text{Đ}_n) / (\text{Đ}_n * (\delta \ln b / \delta \ln w)) \quad (1)$$

where δln b / δln w is the slope of the biovolume spectrum. Trophic levels were computed for the size range 0.6–2.0 mm equivalent spherical diameter, which is dominated by *C. finmarchicus*, 0.6–1 mm encompasses CII-CIII copepodites of *C. finmarchicus* and 1–2 mm encompasses the older copepodite stages CIV, CV and adults. The assimilation efficiency Đ_n was assumed to be 70 %, assuming that a different Đ_n changes the trophic level only slightly (Basedow et al., 2010). Please note that equation 1 differs from the equations to compute trophic level printed in Basedow et al., (2010,2016), those were printed incorrectly.

2.5.2. Stable isotope analyses

From the two bongo net samples at the stations, in total 30 older stages of *Calanus* (CIV to females) and 6 cod larvae were randomly selected for analysis of stable isotopes. No cod larvae were selected from stations P5 to P8 and B1, due to low abundances there. Most unfortunately, precise station labels were lost but samples from inside the fjord (P1 to P8) could be distinguished from shelf station samples (B1 to B3). The six samples from the preceding winter were collected and analysed following the same procedure. The plankton samples were freeze-dried and ground into a homogeneous powder, then treated with cyclohexane to remove lipids. Stable isotope measurements were performed with a continuous-flow isotope-ratio mass spectrometer (Delta V Advantage, Thermo Scientific, Bremen, Germany) coupled to an elemental analyser (Flash EA1112 Thermo Scientific, Milan, Italy) at the University of La Rochelle (LIENSs laboratory). Results were expressed in parts per thousand (‰) relative to Vienna PeeDee Belemnite and atmospheric N_2 for $\delta^{13}C$ and $\delta^{15}N$, respectively, using to the equation:

$$\delta X = ((R_{sample}/R_{standard}) - 1) * 1000 \quad (2)$$

where X is ^{13}C or ^{15}N and R is the isotope ratio $^{13}C/^{12}C$ or $^{15}N/^{14}N$, respectively. The measurement precision was estimated to be of 0.04 ‰ and 0.07 ‰ for $\delta^{13}C$ and $\delta^{15}N$, respectively.

2.5.3. Lipid and fatty acid trophic marker analyses

For the analyses of lipids, the following individuals were selected from the bongo net samples, depending on available time and abundance: at station P1 5 cod larvae, P2 5 cod larvae, P3 17 *Calanus* females and 3 cod larvae, P4 5 cod larvae, P5 18 *Calanus* females, P7 18 *Calanus* females, P8 20 *Calanus* females, B2 14 *Calanus* females and 5 cod larvae, B3 21 *Calanus* females.

The extraction of lipids and separation of individual fatty acids (FA) and fatty alcohols (FAlc) of copepods and cod larvae was conducted at the Alfred Wegener Institute, Germany. Lipids from freeze-dried samples were extracted using a modified procedure from Folch et al. (1957) with dichloromethane/methanol (2:1, v/v) and a washing procedure with an aqueous KCl solution (0.88 %). For quantification of FAs and FAlcs, tricosanoic acid (23:0) was added as an internal standard prior to extraction. The lipid extract was re-dissolved in dichloromethane and taken for analysis or kept at − 20 °C for further analyses. For the gas–liquid chromatography analyses of FAs and FAlcs, aliquots of the total lipid extract were derivertized under nitrogen atmosphere in methanol containing 3 % concentrated sulphuric acid and transesterified for 4 h at 80 °C. After a subsequent cyclohexane extraction, the resulting fatty acid methyl esters (FAMEs) and free fatty alcohols were separated with an Agilent 6890 N Network gas chromatograph (Agilent Technologies, USA) on a 30 m DB-FFAP column (0.25 mm I.D., film thickness: 0.25 μm) equipped with a split injection and a flame ionization detector using a temperature program according to Kattner & Fricke (1986). Helium was used as a carrier gas. FAMEs and alcohols were identified by comparing retention times with commercially available standard mixtures. Total lipid mass per individual was calculated by summing up fatty acids and fatty alcohol masses. The percentage of wax esters in total lipid was calculated from the proportion of alcohols on a mole basis, assuming that copepods contain no free fatty alcohol (Kattner & Krause, 1989). GC mass spectrometry was regularly used to confirm the identification of uncertain lipid compounds.

3. Results

3.1. Water masses

The surface layer inside Vestfjorden consisted of Norwegian Coastal Water (NCW, S < 34.8, Sætre, 2007) and was characterized by relatively low salinity (S < 34.1) and low temperature (T < 5 °C), indicative of freshwater runoff from rivers due to snow melt (Fig. 2). The most pronounced surface layer was observed at the innermost transects S1 and S2, due to the accumulation of runoff in this area. Along all transects, this relatively cool and low saline water extended deeper in the water column at the Northwest side of Vestfjorden compared to the Southeast side. At S4, the differences between the two fjord sides were most pronounced, with fresher, colder water being more prevalent on the Northwest side, indicative of an outflow along this fjord side. The warmest water of all transects was observed at the two outer transects S4 and S5 (Table 1), least influenced by cold freshwater. Warm, saline Atlantic Water (AtW, defined as S > 35, Sætre, 2007) and modified Atlantic Water (mAW, 34.8 < S < 35.0, Sætre, 2007) occupied the deeper layers in Vestfjorden, below ca. 175 to 200 m (Table 1),

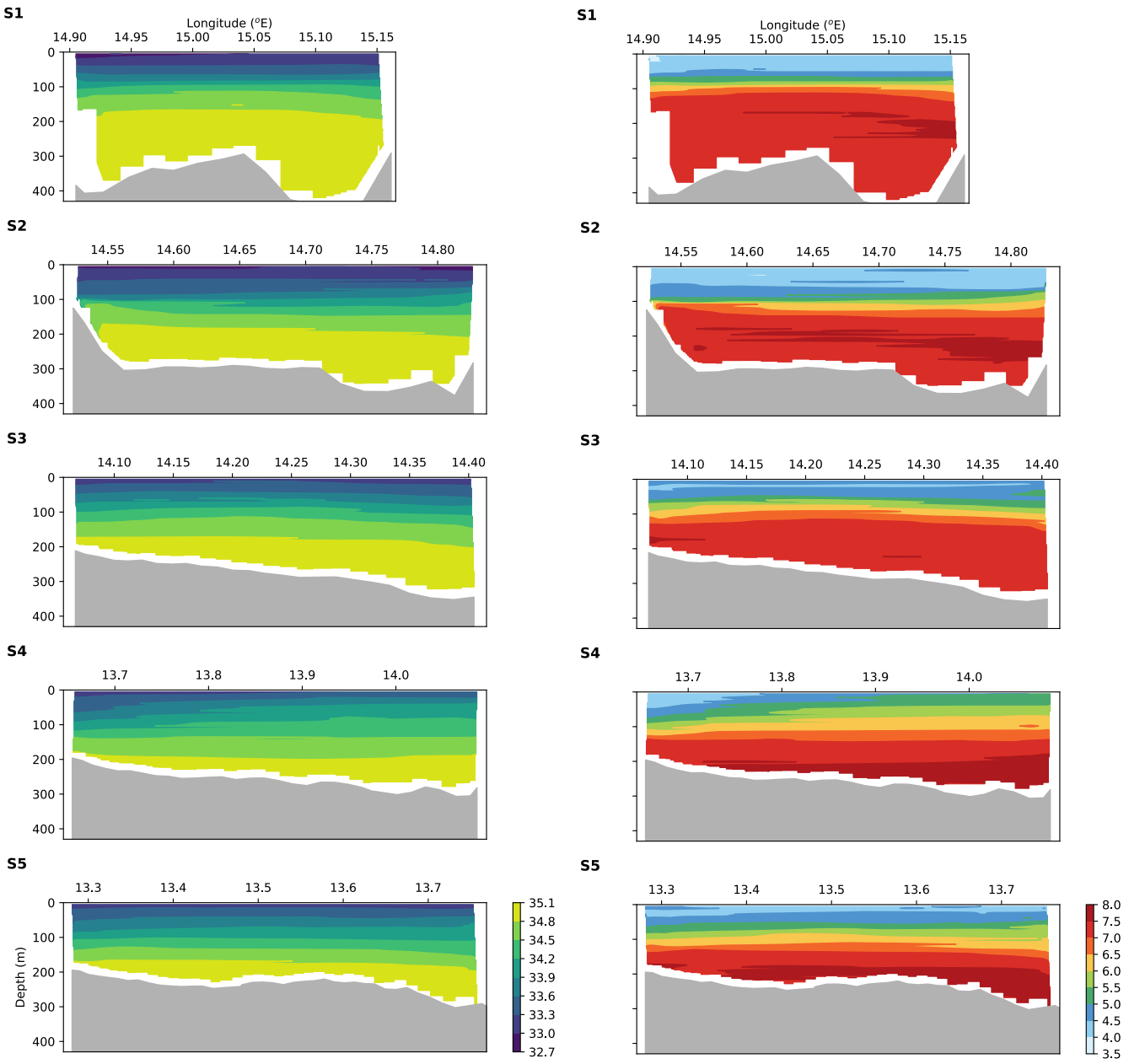

Fig. 2. Practical salinity (left) and *in situ* temperature (°C, right) along transects S1 to S5 in Vestfjorden. Based on data collected in April 2015.

Table 1
Water layers in Vestfjorden, April 2015. Surface layer defined as S < 34.1. ΔT is calculated as the difference in temperature between adjacent water layers, each layer one meter thick.

Transect	Depth of ΔT > 0.005 °C m^{-1} (m)	Thickness of layer with S < 34.1 (m)	Depth of S > 34.8 (m)	Max T in profile (°C)	Max S in profile (psu)
S1	145	97	175	7.48	35.07
S2	174	117	192	7.49	35.06
S3	156	87	178	7.43	35.04
S4	183	73	197	7.54	35.02
S5	172	95	176	7.54	35.04

indicative of a deep inflow of Atlantic water masses at the Southeast side of the fjord (Fig. 2). The saltiest water was observed in the deep, inner part of the fjord (S1 and S2, Table 1), pointing to a restricted exchange of water in this deep part.

In general, a very gradual increase in density with depth was observed in Vestfjorden, with no clear pycnocline. Based on density or buoyancy it was therefore not possible to define the mixed layer depth with confidence. The only exception was the innermost transect S1, where a very shallow mixed layer was observed. Instead, observed temperature gradients and salinity were used to define layers (Table 1). S4 was the shallowest section but had the thickest intermediate layer (34.1 < S < 34.8), as well as the lowest maximum salinity and the temperature gradient started deepest, all pointing to most intense mixing at this transect.

Along the transects crossing from the shelf to the oceanic areas, four main water masses were observed (Fig. 3): NCW occupied the whole water column in the eastern parts and gradually shallower parts further west. Below NCW, mAW and AtW (S > 34.8, T > 0 °C) were present in a thick layer down to ca. 700 – 800 m, below this layer Norwegian Sea Deep Water (S < 35.0, T < 0 °C, Østerhus et al., 1996) was observed. At the northern shelf transect S7, NCW stretched all the way to the western end of the transect, confined to a thin layer above AtW. In turn, AtW

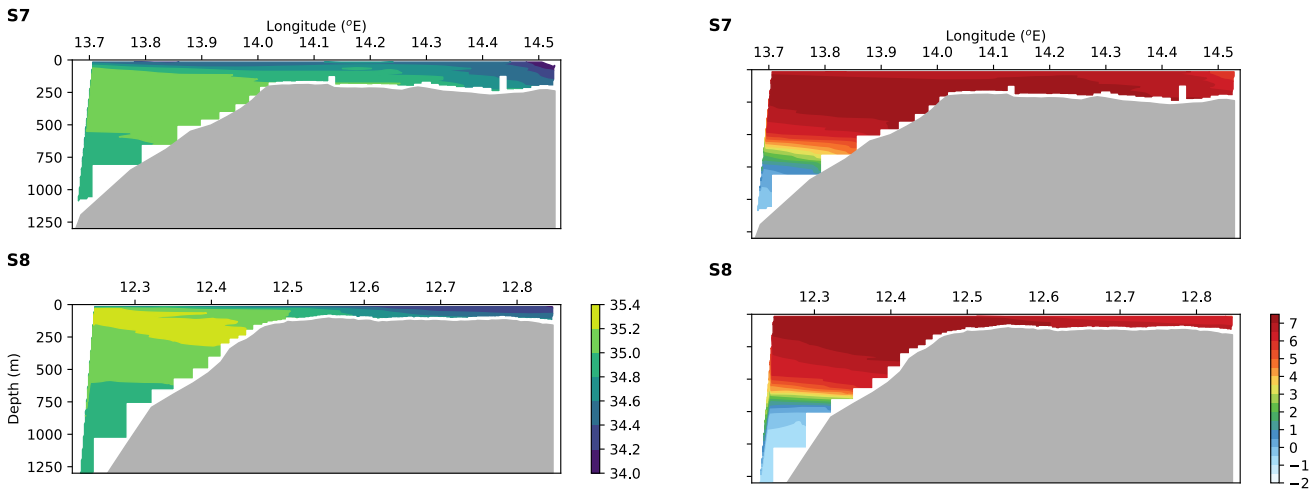

Fig. 3. Practical salinity (left) and *in situ* temperature (°C, right) along transects S7 and S8 across the shelf outside Lofoten islands, sampled in April 2015. Coastal end on right hand side of panels, offshore end on left hand side.

intruded onto the shelf and extended far east on S7, while it was mostly confined to the shelf break along S8. Hence, the front between NCW and AtW was much further west along the southern transect S8 than at transect S7.

3.2. Wind and ocean circulation in Vestfjorden

Wind was blowing from the Northwest prior to our survey, but direction changed to southwesterly winds just before our first sampling (19 April mid-day). During the whole time in Vestfjorden (19–22 April), southwesterly/westerly winds were prevailing (6.5–13 m s^{-1}). On the shelf, northeasterly/easterly winds (6.5–11 m s^{-1}) dominated during the last two sampling days. This shift from southwesterly to northeasterly winds is typical for the summer half-year (mid April to mid September) when wind tends to blow from both directions in equal proportion (Sætre, 2007). Circulation in the fjord was analysed for the wind-influenced surface layer ($S < 34.1$) and the deep layer ($S > 34.8$).

Quite variable flow was observed in Vestfjorden, based on de-tided ADCP data (Fig. 4). In the surface layer, the only more or less clear signals observed were a recirculation at the innermost transect S1 and a push of surface water towards the southeast at the outermost transect S5. The recirculation at S1 might belong to a cyclonic eddy, however, no lifting of the pycnocline in the centre of the transect was observed (Fig. 2). The southeastward push of water at S5 might be responsible for the observed slight deepening of the colder, fresher surface layer there (Fig. 2). At S3, surface water was pushed towards the northwest, resulting in a deepening of the surface layer there. At this transect, a doming of the isopycnals was observed, which could be indicative of an eddy. At the outer transect S5, mean inflow velocity v in the upper layer was 0.04425 m s^{-1}.

In the deeper layer, mean inflow velocity at S5 was 0.04759 m s^{-1}. A clear inflow along the southeastern shore was visible in S5 and S3, and likely existed further southeast of S4 (Fig. 4). Along S2, this inflowing current turned to the northwest for recirculation, where it met shallower bathymetry. This corresponded to a shoaling of isopycnals and warmer, saltier water higher up in the water column at the northwestern end of S2 (Fig. 2). The dip in isopycnals, especially isotherms, in the middle of S2 thus resulted from a combination of freshwater flux from S1, inflow of saltier water from the Southeast and shoaling of the deep layer at the northwestern end.

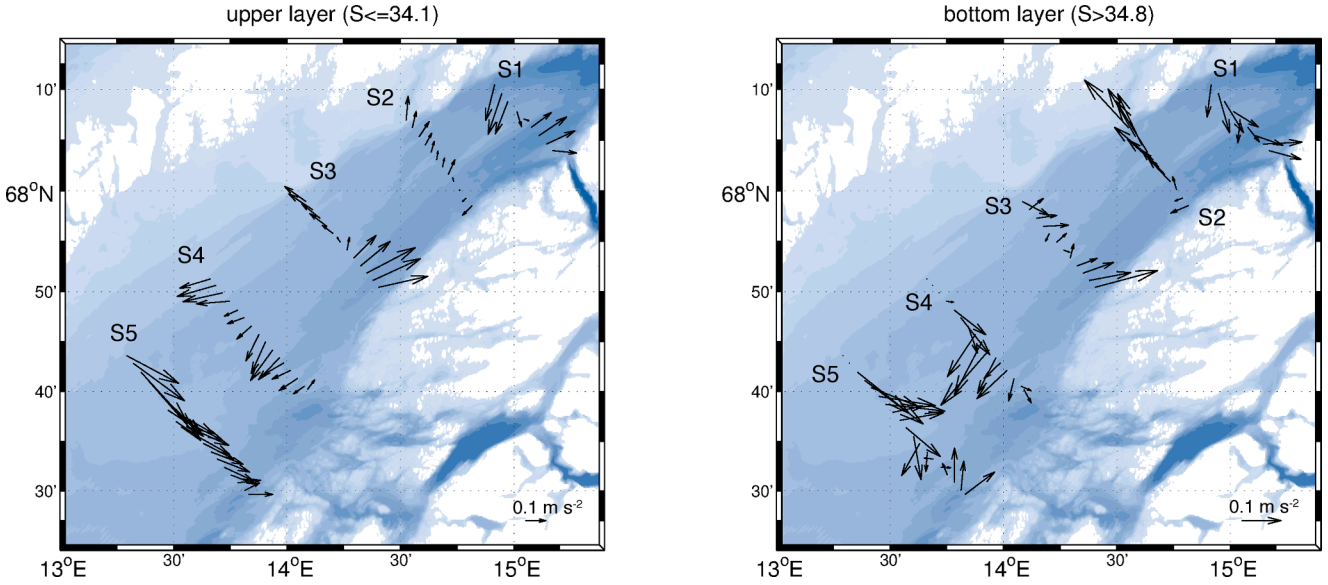

Fig. 4. De-tided currents based on data collected by a ship-mounted ADCP along transects S1 to S5 in Vestfjorden, April 2015. Left: currents in the upper layer, defined by salinity <= 34.1, right: currents in the bottom layer, defined by salinity > 34.8.

3.3. *Calanus* distribution and advection

The distribution of older stages (CIV to adults) of *Calanus* in Vestfjorden was strongly heterogeneous along all transects. Highest abundances of these copepods were mostly, but not exclusively, observed below 100 m (Fig. 5, left panels). This contrasted with the distribution of young copepodite stages (CI-CIII), which were concentrated in the upper layers (section 3.6). Along the transects crossing the shelf (Fig. 5, right panels), higher abundances of older stages were generally observed on the shelf compared to deeper waters off the shelf. However, off the shelf at S7, a patch of relatively high abundances (ca. 2500 ind. m^{-3}) was observed at overwintering depths (ca. 800 m) below AtW (Fig. 3). At the shelf break in AtW (ca. 14 °E) a patch of high abundances of older stages was observed at intermediate depth just below 100 m.

In Vestfjorden, there was a higher probability to observe high abundances of older stages in the deeper, Atlantic-influenced water mass ($S > 34.8$) than in the water mass influenced by river runoff ($S < 34.1$), Fig. 6. High abundances of older stages at depth were observed both in areas where currents were flowing into Vestfjorden and in areas with outwards directed currents (Fig. 4 right panel, Fig. 5 left panels). Looking at the flux of copepods across transects (Fig. 7) in combination with the distribution of copepods (Fig. 5, left) and with the measured

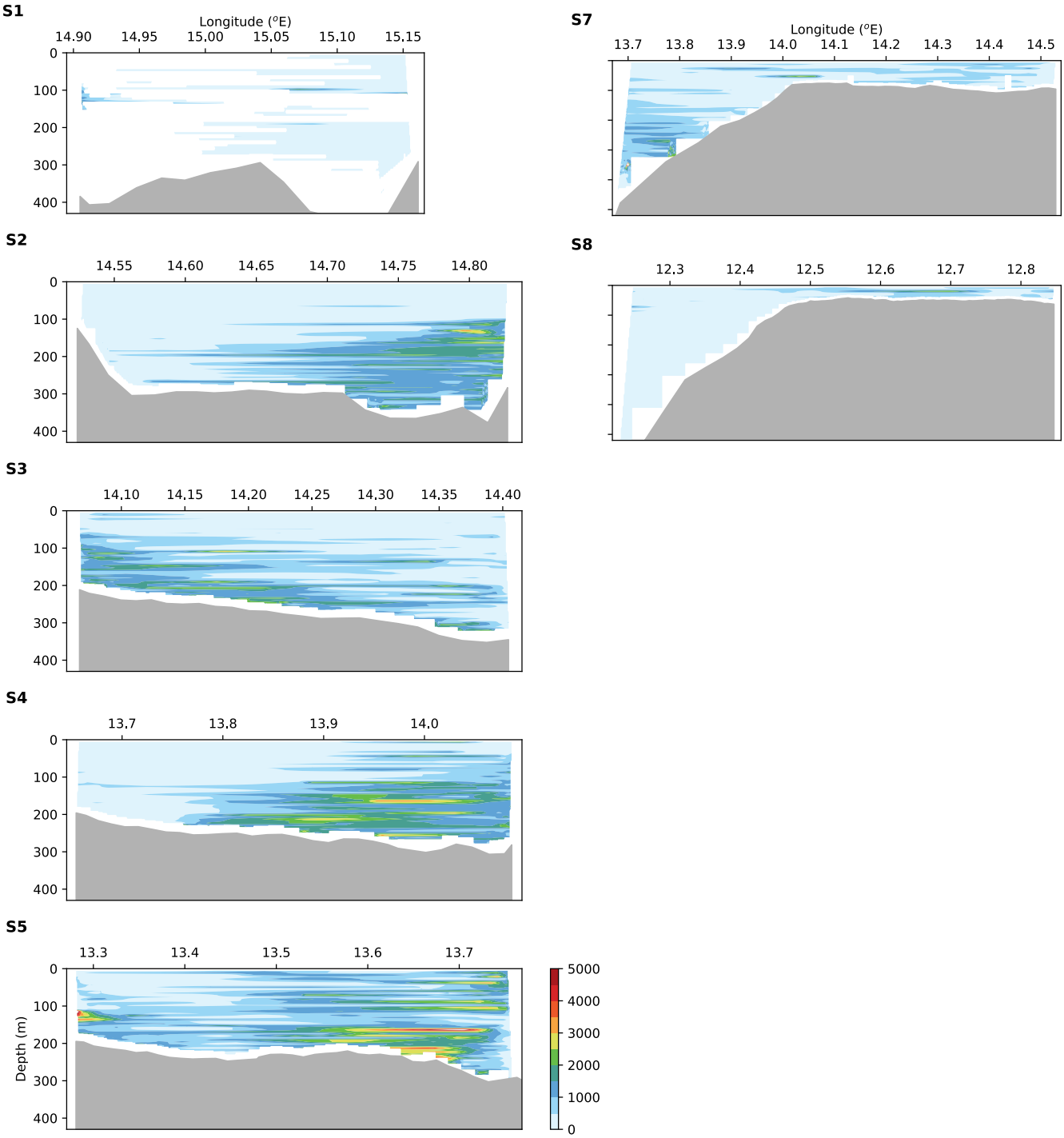

Fig. 5. Abundance (ind. m^{-3}) of older *Calanus* stages (CIV to adults) along transects S1 to S5 inside Vestfjorden (left panels) and S7 and S8 across the shelf outside Lofoten island (right panels). Based on data collected by a Laser Optical Plankton Counter mounted on a Moving Vessel Profiler in April 2015.

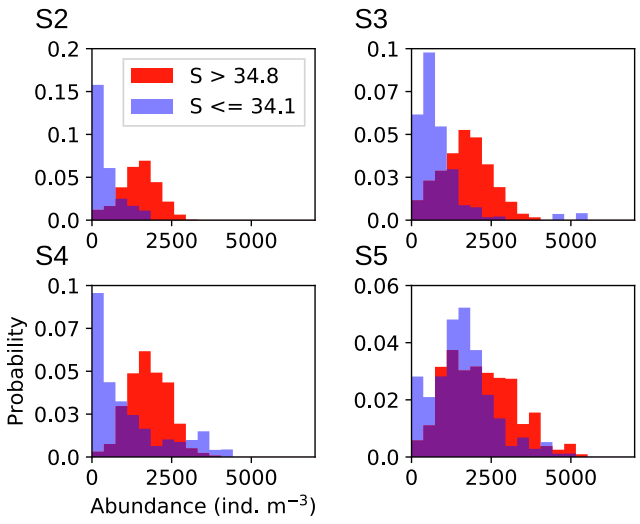

Fig. 6. Probability (y-axis) to observe certain abundances (x-axis, ind. m^{-3}) of older *Calanus* stages (CIV to adults) in Atlantic-type Water (S > 34.8, red) and Coastal Water (S < 34.1, blue). Based on data collected along transects S2 to S5 crossing Vestfjorden in April 2015.

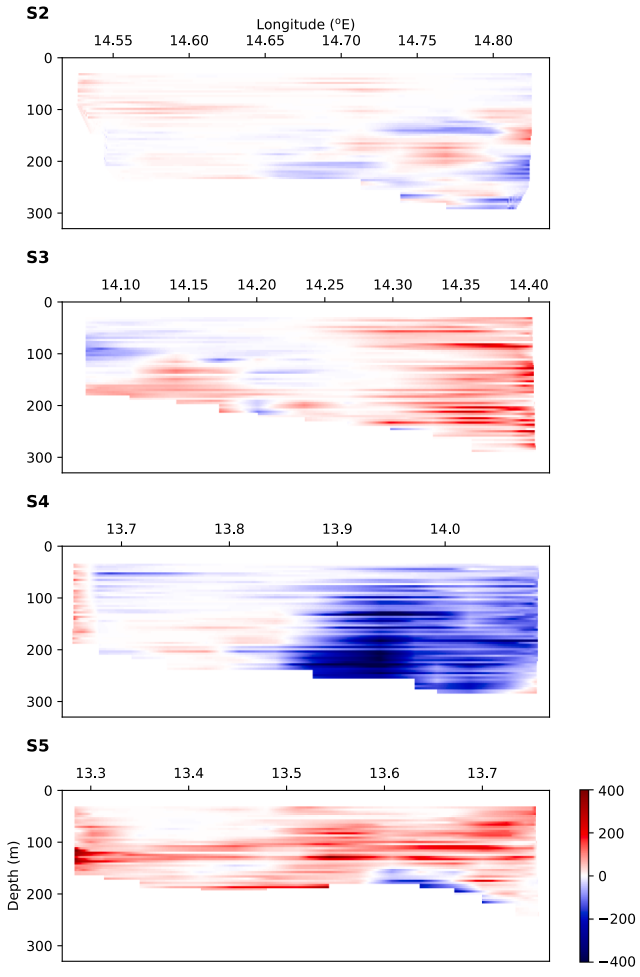

Fig. 7. Flux (ind. m^{-2} s^{-1}) of older *Calanus* stages (CIV to adults) across transects S2 to S5 in Vestfjorden, April 2015. Negative values (blue) = flux out of the fjord, positive values (red) = flux into the fjord.

currents (Fig. 4), we can trace patches of copepods through the fjord to elucidate their origin from inside or outside of the fjord. The high abundances across the water column east of ca. 13.7 °E at the southernmost transect S5 (Fig. 5) matched with an observed inflow across the water column (Fig. 4), thus resulting in a flux of up to 400 copepods m^{-2} s^{-1} into Vestfjorden (Fig. 7). At S4, we observed an inward flux of copepods at the very eastern end at depth (Fig. 7), however, most of the inflow in all likelihood happened further southeastward and closer to the shore than our observations. The inflow of copepods with the inflowing current along the southeastern shore was also observed at S3 (Fig. 7), however at this transect the inflow was not restricted to the inflowing current. Instead, there was an inward flux along the entire transect (Fig. 7), corresponding to inward currents along the entire transect (Fig. 4) and patches of high abundances at ca. 200 m at the northwestern end of the transect as well as spread patches across the water column east of ca. 14.3 °E (Fig. 5). At S2, the flux of copepods was more mixed (Fig. 7), but inflowing patches were observed, east of ca. 14.7 °E at ca. 200 and ca. 150 m, respectively (Fig. 5). At S2 the inflowing current recirculated and was forced to flow upward due to a shoaling in bathymetry (Fig. 4, see also section 3.2). This corresponded with an outward flux of ca. 100 copepods m^{-2} s^{-1} at about 100 m at the northwestern end of S3 (Fig. 7).

The observed doming of isopycnals at S3 at ca. 14.2 °E (Fig. 2), possibly indicating a cyclonic eddy in that area, matched with patches of high abundances relatively high up in the water column, at about 100 m at 14.2 °E (Fig. 5, S2). Also observed fluxes at the outermost transects S4 and S5 are in agreement with circulation patterns within an anticyclonic eddy: high abundances below 100 m (Fig. 5) were observed both in areas with inward and outward directed water currents (Fig. 4). This resulted in high (up to 400 ind. m^{-2} s^{-1}) fluxes of copepods both into and out of Vestfjorden (Fig. 7).

3.4. Zooplankton and ichthyoplankton at the stations

The morphological analyses of the zooplankton community at all stations revealed a dominance by *C. finmarchicus*. Within the upper 30 m, young *C. finmarchicus* (CI-CIII) were found in abundances an order of magnitude higher than all other taxa combined (other taxa not shown). Maximum CI-CIII abundances (10,000 to 11,000 ind. m^{-3}) were observed at stations P4 in the middle of transect S4 and B3 on the shelf (Fig. 8). Only a few other taxa occurred in abundances higher than 100 ind. m^{-3}, among these were meroplanktonic larvae (Polychaeta, Cirripedia and Decapoda zoea larvae) and Ostracoda. Small copepods (*Oithona* spp., *Microcalanus* spp., *Pseudocalanus* spp., *Triconia borealis*, *Acartia longiremis*) mostly had abundances < 10 ind.m^{-3}, with the exeption of *Oithona similis* (maximum abundance 142 ind. m^{-3} at P4). Of medium-sized copepods only *Metridia longa* occurred throughout the fjord, albeit in low densities (maximum 1.3 ind. m^{-3} at P4). Below 30 m, zooplankton abundances were generally low, and dominated by older *Calanus* stages (CIV to adults).

In the upper layer in Vestfjorden, the *Calanus* population was predominantly centered around copepodite stage CII, with the least advanced population (stage index 1.6) observed at the outermost station P1 (Table 2). On the shelf, the population development was slightly more advanced, with stage indices between 2.3 and 2.9. Nauplii abundances were generally low, especially at the stations P1 and P7, and at the southernmost station on the shelf, B1. Highest nauplii abundances were observed at the shelf stations B2 and B3 (Table 2), coinciding with highest abundances of CI-CIII stages (Fig. 8). Copepodites CI-CIII were mostly concentrated in the upper 20 m but occurred with relatively high abundances down to 100 m at P5 and P7 (Fig. 8). Low abundances of fish eggs and larvae were observed in the net samples (Table 2).

3.5. Phytoplankton development

The 10-year time-series of surface (5 m) chl *a* fluorescence data

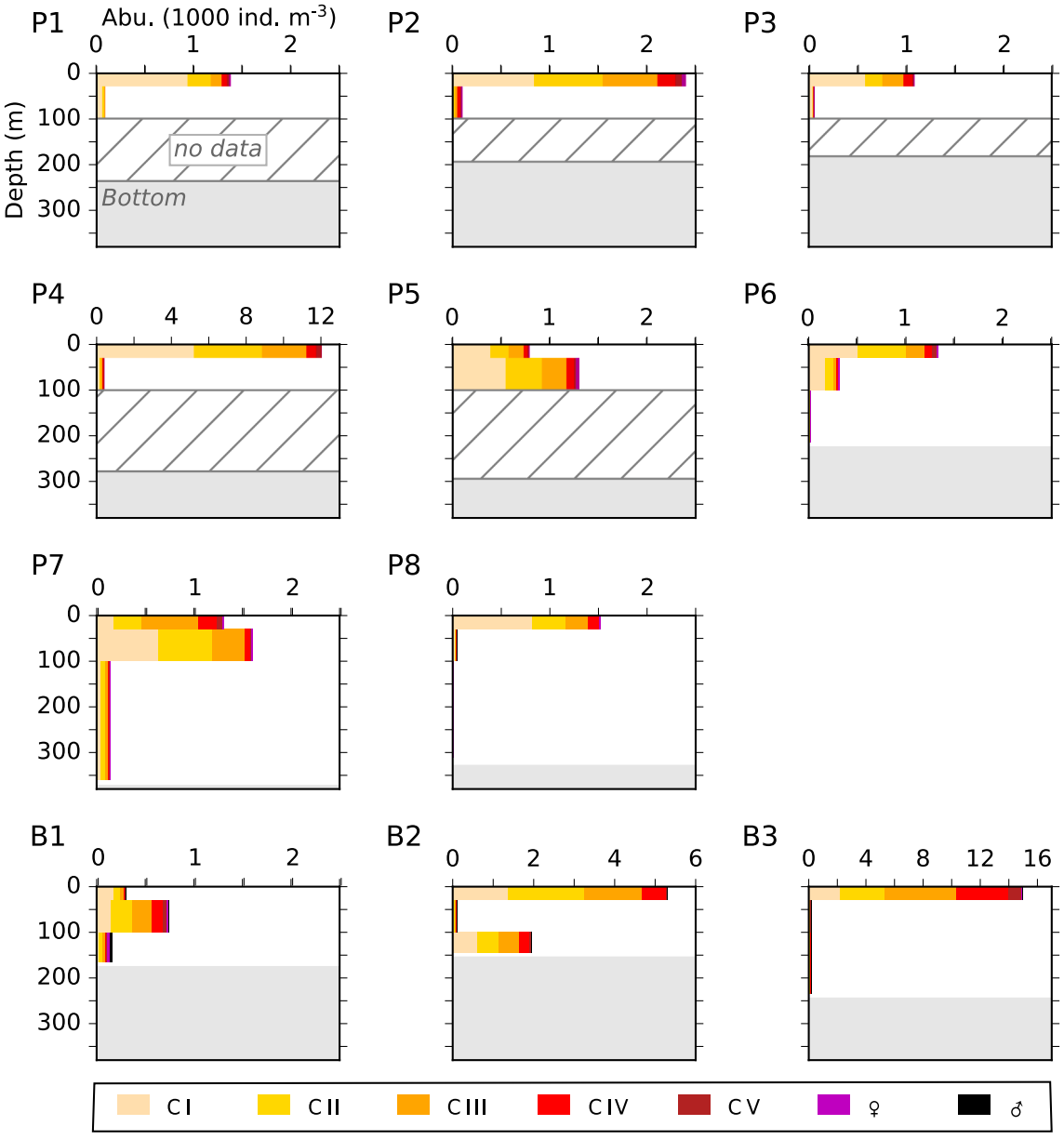

Fig. 8. Vertical distribution and abundance (Abu., 1000 ind. m^{-3}) of *Calanus* developmental stages CI to adults. Based on vertically stratified data collected by a WP2 net (180 μm) at eleven stations in Vestfjorden (P1 to P8) and on the adjacent shelf (B1 to B3) in April 2015.

collected by the FerryBox crossing the fjord shows a remarkably consistent start of the phytoplankton bloom at the end of March, which then culminates around April 11 (Fig. 9). The bloom starts in the East and is a few days delayed in central and western parts of the fjord. A second and much smaller bloom at the end of May is evident in the time-series; it is more pronounced along the southeastern shore of the fjord. During our cruise at the end of April, we determined nutrients that were nearly depleted in the upper layer inside the fjord, as well as subsurface maxima of chl *a* (Table 3), both indicative of a situation at the end of the bloom. The deepest chl *a* maxima, around 40 m, were observed in the middle of the fjord, at stations P5 and P6. At the southernmost shelf station B1, the depth of the chl *a* maximum resembled the situation inside the fjord, while no pronounced chl *a* maximum was observed at B2 and a shallower maximum at 15 m at B3.

3.6. Trophic flow

Biovolume spectrum analyses revealed relatively constant trophic levels of the zooplankton community dominated by *C. finmarchicus* inside the fjord (Fig. 10). Estimated trophic levels ranged between 1.8 and 2.4 at stations P1 to P8. Slightly but significantly lower values were calculated for the stations close to the northern shore of the fjord (P2, P3, P6, P8; mean = 1.83, SD = 0.05) compared to the stations in the middle of the fjord (P1, P4, P5, P7; mean = 2.20, SD = 0.18), t(3.4) = 3.6, p = 0.02. At the stations B2 and B3 on the shelf, very low trophic positions of 1.3 and 1.5, respectively, were calculated (Fig. 10, Table S3).

In winter, no coast-shelf differences were observed among the *Calanus* individuals: stable $\delta^{15}N$ and $\delta^{13}C$ isotope values of older stages (CIV to adults) were very similar in Vestfjorden (8.6 and −21.9, respectively) and on the shelf (8.9 and −21.9), with a low variance between stations (Fig. 11). In contrast, both $\delta^{15}N$ and $\delta^{13}C$ isotope values of older *Calanus* stages differed between Vestfjorden and the shelf in spring. Then, stable $\delta^{15}N$ values in Vestfjorden (7.3) remained similar to winter values (8.6), whereas on the shelf a pronounced decrease in $\delta^{15}N$ values (5.7) was observed compared to winter values (8.9). At both locations in spring,

Table 2
Calanus and ichthyoplankton. A. Abundance of ichthyoplankton and *Calanus* nauplii at eight stations in Vestfjorden (P1 to P8) and three stations on the shelf (B1 to B3), sampled in April 2015. B. Relative abundance of *Calanus* developmental stages based on 180 μm net samples integrated over the upper 100 m (P1 to P5) or from bottom to surface (other stations). nd = no data, – = none observed.

	P1	P2	P3	P4	P5	P6	P7	P8	B1	B2	B2
A. Abundance (individuals m^{-3})											
30–0 *m*											
Nauplii	29	nd	301	nd	245	nd	31	nd	89	495	319
Fish eggs	37	24	16	4	14	26	85	24	0.1	21	75
Cod larvae	6	0.9	0.8	3	3	3	8	3	1	13	35
100–30 *m*											
Fish eggs	1	0.6	2	0.1	2	0.2	14	0.4	0.1	0.7	5
Cod larvae	0.2	0.1	0.1	0.4	0.4	0.1	0.3	–	0.1	0.1	1
B. Relative abundance (%)											
CI	67.8	33.9	54.2	43.1	44.8	41.0	27.7	53.6	28.4	27.3	14.9
CII	17.5	28.8	15.6	29.7	26.6	35.4	29.3	21.9	27.1	32.8	20.8
CIII	8.2	23.4	19.1	19.7	19.4	13.2	30.9	15.3	22.5	26.5	33.4
CIV	3.9	8.7	8.3	4.6	5.8	6.0	8.9	7.4	11.8	11.7	24.3
CV	1.4	3.0	1.4	2.7	1.4	3.0	2.3	0.6	4.3	1.2	6.1
AF	1.1	2.3	1.4	0.1	2.1	1.4	0.9	1.2	3.4	0.3	0.6
AM	0.0	0.0	0.0	0.0	0.0	0.0	0.0	0.01	2.6	0.2	0.1
Stage index	1.6	2.3	1.9	1.9	2.0	2.0	2.3	1.8	2.5	2.3	2.9

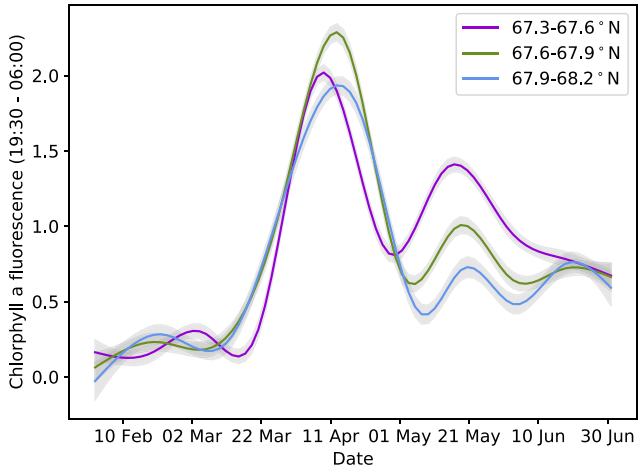

Fig. 9. Seasonal development of chl *a* fluorescence (10-year average, mg/m^{-3}) in Vestfjorden, shown for three different regions of the transect sampled by the FerryBox from Bodø to Stamsund. Grey shadows indicate confidence intervals. Night data (19:30–06:00 UTC) were used to remove the effects of the diurnal variation in the chl *a* fluorescence.

$\delta^{13}C$ isotope values varied among stations (SD of 0.9 in Vestfjorden and 0.5 on the shelf). In Vestfjorden, the large variance in $\delta^{13}C$ isotope values between stations is due to two groups in the data: four stations had a stable mean $\delta^{13}C$ value of –22.5 and three stations a mean value of −20.8. On the shelf, no evidence of a trophic link between older *Calanus* stages and local phytoplankton was observed: there was a significant difference between $\delta^{13}C$ values of POM (–23.5) and of copepods (−19.4) in spring (Fig. 11).

All *Calanus* females showed similar fatty acid and fatty alcohol profiles, with higher levels of the biomembrane fatty acids 16:0 (12–19 %), 20:5(n-3) (15–20 %) and 22:6(n-3) (9–16 %, B3: 22 %) and low levels of the diatom marker 16:1(n-7) (4–7 %), the dinoflagellate marker 18:4(n-3) (7–10 %) and the *de novo* biosynthesized FAs 20:1(n-9) (4–7 %) and 22:1(n-11) (4–8 %), Table 4. Smaller amounts were determined of the fatty acids 16:3(n-4) (1–2 %), 16:4(n-1) (1–3 %), 18:0 (2–7 %) and 18:1(n-9) (1–3 %). The *Calanus* females from stations P2, P3 and P5 had relatively high wax ester levels between 35 % and 54 %, similar to those at stations P7, P8, B2 and B3 (33–66 %), Table 4. *Calanus* females from P5 had a low wax ester content of 15 %. Across stations within Vestfjorden (P3, P5, P7, P8), the ratio of 22:1/20:1 fatty alcohols, ranging from 6-9 % and 4–6 % respectively, remained approximately 1 across all samples. On the shelf (B2, B3) and at the outermost station in Vestfjorden (P2) *Calanus* females had very high levels of the 20:1 and 22:1 fatty alcohol isomers (27–31 % and ca. 44 %, respectively) with a 22:1/20:1 ratio of 1.6 for P2 and 1.4 for B2 and B3.

The cod larvae from stations P2, P3 and P4 had high levels of wax esters (44–56 %), with a fatty alcohol ratio of 22:1/20:1 of approx. 1.8 at stations P2 and P3 and 0.9 at station P4, Table 4. Lower levels of wax esters (ca. 7 %) were recorded at P1 and B2. Cod larvae from P2, P3 and P4 had similar fatty acid compositions with higher concentrations of 16:0 (15–18 %), 16:1(n-7) (6–9 %), 20:5(n-3) (15–19 %) and 22:6(n-3) (11–17 %), while cod larvae from P1 and B2 had higher levels of 16:0 (22–24 %), 18:0 (11–14 %), and 22:6(n-3) (24–25 %). Moderate concentrations of the long-chain monounsaturated FAs occurred in the wax ester-rich specimens (20:1(n-9) and (n-7): 4–8 %, 22:1(n-11): 5–6 %).

4. Discussion

4.1. *Calanus* advection

The distribution of *Calanus* appeared to be mostly linked to the advection of modified Atlantic Water (mAW) into the fjord and based on the high-resolution data of water masses and copepods we could distinguish patches of high *Calanus* abundance and trace these throughout the fjord system. The results support the view that inflowing copepods from the south greatly contributed to the Subarctic fjord ecosystem in spring. The measured inflow of up to 400 *Calanus* ind. m^{-2} s^{-1} into the fjord corresponds to roughly 60 mg C m^{-2} s^{-1}, assuming a mean carbon content of 150 μg $ind.^{-1}$ for the older developmental stages (CIV to adults) of *Calanus* (Hygum et al., 2000). Along the fjord entrance (transect S5), about 795 000 ind. s^{-1}, or 119 g C/s, entered the fjord with the inflowing current.

To assess in how far this advective inflow of *Calanus* controls biomass formation in the fjord, we can calculate the advective rate β and compare it to the local growth rate *r* (Aksnes et al., 1989).

$$\beta = 0.5 \times v \times (A/V) \quad (3)$$

with *v* = mean inflow velocity (m/s), A = cross sectional area (m^2), V = fjord volume (m^3). For Vestfjorden in April this results in a β of 2.9 x 10^{-7} s^{-1}. At 4 °C, the growth rate *r* of *Calanus* is in the order of 1.5 x 10^{-6} s^{-1} under non-limiting food conditions (Campbell et al., 2001). The ratio r/β was > 0 (5.2), indicating that local prosesses dominated during our study period. This rough comparison is based on a relatively low inflowing current velocity (0.045 m s^{-1}) that was observed across the

Table 3
Nutrient and chlorophyll *a* concentrations at stations in Vestfjorden (P1 to P8) and on the adjacent shelf (B1 to B3), April 2015. The depth of the chlorophyll *a* maximum (Chl max dep) is also shown. – = below detection limit or not sampled, nd = no data available. See Fig. 1 and Table S1 for location of stations.

A. Nutrient concentration (mmol/m^{-3}(–|-))												
Depth (m)	**NO3$^-$/NO2$^-$**			**NO2$^-$**			**Si(OH)4**			**PO4^{3-}**		
	'P7'	'P5'	'P4'	'P7'	'P5'	'P4'	'P7'	'P5'	'P4'	'P7'	'P5'	'P4'
0/1	0.1	0.2	0.4	–	–	–	0.46	0.40	1.14	0.07	0.01	0.01
5	0.1	0.3	0.1	–	–	–	0.53	0.49	1.12	0.10	–	–
10	0.5	0.2	0.1	0.1	–	–	0.25	0.35	1.16	0.10	–	–
20	1.1	0.4	0.1	–	–	–	0.83	0.43	0.37	0.10	0.01	–
50	4.3	3.3	4.3	0.1	0.1	0.1	1.61	0.88	1.86	0.30	0.02	0.02
Bottom	11.4	12.4	nd	–	–	nd	6.26	5.88	nd	0.85	0.02	nd
B. Chlorophyll *a* concentration (mg/m^{-3}(–|-))												
Depth (m)	**P1**	**P2**	**P3**	**P4**	**P5**	**P6**	**P7**	**P8**	**B1**	**B2**	**B3**	
5	6.6	3.9	2.3	1.2	1.3	2.1	1.1	1.7	4.5	5.2	4.1	
10	–	–	1.9	–	–	–	–	–	–	–	–	
20	–	–	–	–	–	2.4	–	–	–	–	–	
25	–	–	–	–	–	–	1.2	–	–	–	–	
30	–	8.5	–	7.0	1.6	–	–	7.7	5.8	4.8	4.2	
Chl max	11.4	9.5	6.0	10.2	8.6	8.9	12.2	11.7	8.3	–	7.5	
50	9.8	2.0	4.7	7.0	3.1	3.2	5.8	5.4	5.1	4.7	3.9	
100	0.9	4.3	–	1.5	1.1	1.7	4.6	0.5	2.1	3.0	2.8	
173	–	–	0.3	–	–	–	–	–	–	–	–	
Chl max dep	29 *m*	27 *m*	20 *m*	34 *m*	41 *m*	40 *m*	30 *m*	35 *m*	27 *m*	nd	15 *m*	

outer transect S5, it may be higher at times. The growth rate estimate assumes optimal food conditions, which can be provided by the prolonged phytoplankton bloom and will be favourable for local growth of copepods. In the preceding winter (January 2015), a local population of 2.45 x 10^{12} CV (333 metric tons C) was estimated for Vestfjorden, based on net samples from areas < 500 m and > 500 m within the fjord (Espinasse et al., 2016b). Advecting *Calanus* CIV-adults for one month with the same rate as observed during our study (119 g C/s) would yield an advected biomass of 312 metric tons C. Concluding, the advection accumulates copepods in the fjord but if local growth conditions are optimal local growth prosesses will control biomass formation in the fjord, despite the large fjord opening. The Atlantic input of older copepods into Vestfjorden in April is comparable to the advection of older developmental stages of *C. finmarchicus* into Kongsfjorden, an Arctic fjord further north along the pathway of mAW, which was ca. 1 million ind. s^{-1} in May (Basedow et al., 2004). Compared to the biomass of *Calanus* that is advected into the large downstream seas, Barents Sea (ca. 100 kg C/s in June) and Arctic Ocean (ca. 34 kg C/s in May), the advection of copepods into the fjord systems is about one order of magnitude lower (Edvardsen et al., 2003, Basedow et al., 2018).

4.2. Ocean-coast exchange – origin of Calanus populations in the fjord and on the shelf

Most of the advected older stages (CIV to adults) in the fjord were located below 100 m. In contrast, in the upper layers the *Calanus* population was centered around copepodite stage CII. This points to two different sources of the *Calanus* population occurring within the fjord: one that is still overwintering and advected in deeper layers, and one that has already ascended and reproduced presumably from local overwintering stocks. Both population parts together will result in a prolonged period over which nauplii are available. At prevailing temperatures in surface waters in the fjord (4 °C) it takes *Calanus* about one month to develop from egg to CII, assuming no food limitation (Campbell et al., 2001). The Norwegian Coastal Current collects cold run-off from snow melt resulting in similar surface temperatures all along the Norwegian coast during the melting period (Sætre, 2007). Hence, CII copepodites observed in NCW around April 20 (our study period) most likely had been spawned around March 20, irrespective of origin. Back-calculated spawning times are in line with the known life cycle of *C. finmarchicus* in the northern Norwegian Sea, where the spawning period of *C. finmarchicus* starts in mid-March in fjords and on the shelf, while it commences two weeks earlier on the southern Norwegian shelf (Diel & Tande, 1992, Arashkevich et al., 2004). This points to a local origin of the young copepodites (G_1) observed in surface waters, from within deep fjords or nearby locations (Espinasse et al., 2016b).

The older developmental stages (G_0), on the other hand, are likely being advected with the inflowing current into the fjord and originate from the Lofoten Basin. Modelling results indicate that cross-shelf advection of overwintering *C. finmarchicus* in the northern Norwegian Sea happens predominantly through the Træna trough south of Vestfjorden (Opdal & Vikebø, 2016). Towards the end of our cruise, around April 23, we observed an intrusion of oceanic AtW far onto the shelf also through the relatively deep channel at the northern section S7, the Hola trough (Bøe et al., 2009). This water mass included high abundances of older stages of *Calanus*, residing at depths around 100 m at the shelf break. Off the shelf, the relatively high abundances of older stages observed at depths > 800 m, below AtW, indicate that the copepods were still overwintering here, matching abundances of overwintering *Calanus* observed in the Lofoten basin (Gaardsted et al., 2010). The ascending of *C. finmarchicus* from overwintering in the deep oceanic basins in the Norwegian Sea is delayed by about one month, compared to Coastal Water, and peaks as late as the end of April (Bagøien et al., 2012, Strand et al., 2020). We thus propose that the older copepods observed in AtW/mAW on the shelf and in the fjord originated from the overwintering population in the Lofoten Basin and had recently been advected into the system. Following known ontogenetic migration patterns, those advected copepods will emerge within the next days and will then feed and reproduce, this way contributing to an extended period of nauplii availability.

Our conclusion on an advective origin of older developmental stages is supported by the $\delta^{13}C$ stable isotope signatures of *Calanus* from the shelf, which differed markedly from the $\delta^{13}C$ values observed for POM at the same stations, indicating that those copepods were not feeding on the same material that was available in the water column or they were not yet feeding at all. The observations are also in line with modelling results indicating that most of the *C. finmarchicus* on the northern Norwegian shelf in spring originate from the Lofoten Basin (Opdal & Vikebø, 2016). In turn, models and observations have also suggested that most of the overwintering *C. finmarchicus* in the Lofoten Basin originate from the Norwegian shelf in late summer and autumn (Slagstad & Tande, 1996, Slagstad & Tande, 2007) and are accumulated at the continental slope throughout winter (Dong et al., 2022). Despite the high advective losses of *C. finmarchicus* to areas downstream, our results thus indicate that a significant part of the population is able to complete its life cycle in the fjord, shelf and oceanic regions of the northern Norwegian Sea.

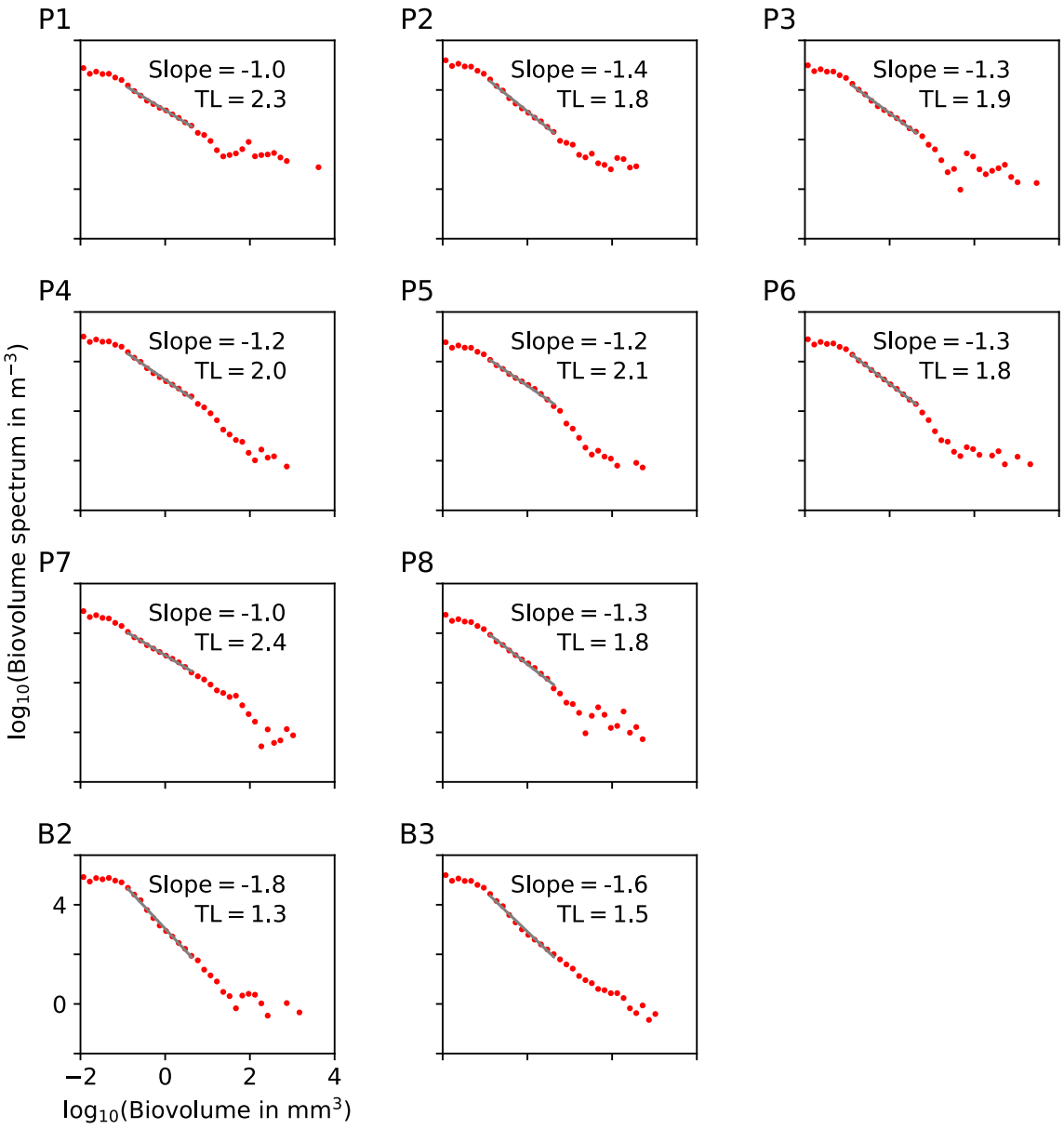

Fig. 10. Biovolume spectra and trophic levels (TL) of the mesozooplankton community at ten stations in Vestfjorden and on the adjacent shelf in April 2015. The slope of the spectrum between 0.6 to 2 mm equivalent spherical diameter (grey line) is given; this size range encompasses copepodite stages CII to adults of *Calanus finmarchicus*. The trophic level was calculated based on the slope, see Methods.

4.3. Retention in the fjord – Modulated by eddies?

We observed a significant inflow of copepods into the fjord, but also flux directed out of the fjord at some transects, and these results are in agreement with the occurrence of eddies within the fjord system. The observed doming of isopycnals at S3 might indicate a cyclonic eddy in that area, and currents and fluxes across S4 and S5 suggests the presence of an anticyclonic eddy in the outer part of the fjord. These *in situ* measurements align well with an earlier study that observed eddies in Vestfjorden based on satellite images of sea surface temperature (SST) and drifter paths (Mitchelson-Jacob & Sundby, 2001). In particular, those authors observed anticyclonic eddies in the outer part and a cyclonic eddy further inside the fjord, matching with our data. A satellite image from April 2015 (Fig. S2) shows a negative SST anomaly in the outer part of Vestfjorden that fits with the relatively thick layer of cold surface waters at S5, compared to S4 (Table 1, Fig. 2) and is in line with an anticyclonic eddy. Point measurements of abundances at stations are rather difficult to directly link to oceanographic data along transects. For example, the high abundances of copepodites observed in surface waters at P4 and P2 could be related to upwelling at the edges of the proposed anticyclonic eddy, but that is hard to ascertain based on our data. In the area of the cyclonic eddy (upwelling on the northern hemisphere), we did observe high abundances of older copepods relatively high up in the water column (Fig. 5, S3, ca. 14.2 °E) and particularly high abundances in surface waters further west in that proposed eddy (Fig. 5, S3, ca. 14.1 °E).

Eddies can retain both zooplankton and fish larvae in fjords (Pedersen et al., 2003, Basedow et al., 2004, Gillibrand & Amundrud, 2007), thus eddies in Vestfjorden could contribute to retaining and concentrating copepods in the fjord, both locally spawned copepods and those entering the fjord with the NCC. For young copepodites to develop locally a relatively long retention time in the fjord system is required, ca. 30 days to develop from egg to CII at 4 °C, as outlined above. At 4 °C, first-feeding cod larvae emerge ca. 25 days after spawning (Pepin et al., 1997). Residence times in Vestfjorden were estimated to be 7–16 days for the months February to April but are likely longer if retention in

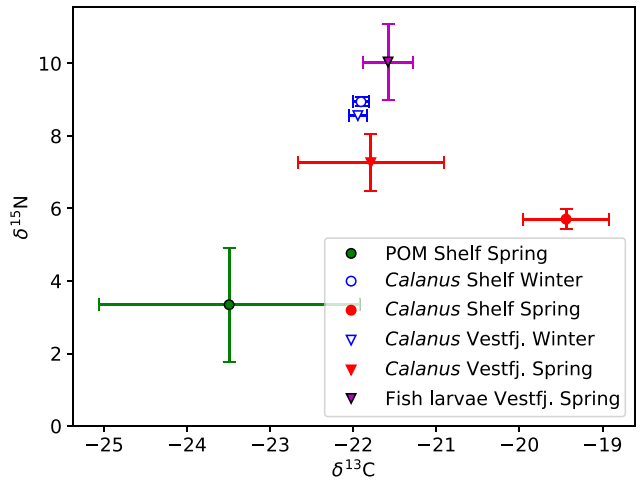

Fig. 11. Stable isotope values of δ^{15}N (y-axis) and δ^{13}C (x-axis) for particulate organic matter (POM), older *Calanus* stages (CIV to adults) and cod larvae in Vestfjorden and on the adjacent shelf.

eddies is included when estimating residence times (Sundby, 1978). Eddies may thus allow for long enough retention times in the fjord system, so that both *Calanus* nauplii and cod larvae can develop in concert. Although several results of our study are in agreement with an increased residence time of copepods in Vestfjorden, further research is needed to ascertain the role of eddies in retaining copepods in this fjord.

4.4. Phytoplankton spring bloom development – enabling match with copepods

The phytoplankton spring bloom system in fjords and on the shelf along the northern Norwegian coast lasts for ca. ten weeks. The 10-year FerryBox data set shows that the spring bloom onset in Vestfjorden started around the vernal equinox (March 21), peaked around April 11 and ended by the end of April, with remarkably low variability between years. This consistency is in line with an analysis of ocean colour remote sensing of chl *a* (Vikebø et al., 2019). Those analyses revealed a more regular start of the bloom along the northern Norwegian coast compared to the southern Norwegian Sea and indicated a peak of the bloom around April 14. On the shelf, the bloom peaks around mid-April as in the fjord, whereas in deeper waters offshore the bloom is delayed and peaks around mid-May (Basedow et al., 2006, Silva et al., 2021, Meng et al., 2023). In Vestfjorden, a second bloom starts in mid-May, peaks around May 20 and ends in the beginning of June. Phytoplankton spring blooms along the northern Norwegian coast tend to be dominated by diatoms of the genus *Chaetoceros* (Degerlund & Eilertsen, 2010). The prolonged bloom phenology in the fjord-shelf system off the northern Norwegian coast can thus provide high-quality diatom food for developing copepod populations over an extended period of time (Schnack, 1979).

4.5. Trophic relationships and match/mismatch of trophic levels

The lower trophic level food web inside the fjord was tightly coupled between phytoplankton, *Calanus* and cod larvae. These appeared to match in space in time. Here, the zooplankton community dominated by *Calanus* had a trophic position around 2, as calculated based on bio-volume spectrum analyses. This low trophic position is indicative of a purely herbivorous feeding and short food chains with very limited cycling through the microbial loop, typical of the spring bloom (Basedow et al., 2016, Heneghan et al., 2016). Those estimates are consistent with the δ^{15}N values of older stages of *Calanus* that remained close to winter values of δ^{15}N, thus indicating a recent start of feeding of these stages. Significantly lower trophic position at the northern shore compared to the inner part of the fjord are in line with a different origin

Table 4
Fatty acid and fatty alcohol compositions (%TFAs) and wax ester (WE) levels (% TFA + Alcohol) of *Calanus* adult females (A) and cod larvae (B). – = not detected. PUFA = polyunsaturated fatty acids, MUFA = monounsaturated fatty acids, SAFA = saturated fatty acids.

A. *Calanus*

	Station						
Fatty acid	P2	P3	P5	P7	P8	B2	B3
14:0	9.0	4.2	4.7	4.4	3.0	8.6	4.1
16:0	15.6	14.0	18.2	18.9	13.3	11.8	17.1
16:1(n-7)	7.3	6.9	6.8	5.2	5.5	6.5	3.9
16:2(n-4)	–	0.7	–	0.5	0.2	0.8	0.5
16:3(n-4)	1.5	1.4	1.1	0.8	0.9	2.1	0.9
16:4(n-1)	2.9	1.6	1.3	0.9	1.1	4.7	1.3
18:0	7.0	2.2	6.8	4.0	2.3	2.0	3.0
18:1(n-9)	2.0	2.9	3.4	1.8	3.4	0.8	1.4
18:2(n-6)	1.0	1.2	1.7	0.2	1.8	0.2	1.1
18:4(n-3)	6.7	7.8	6.5	7.5	10.3	10.3	9.2
20:1(n-9)	5.9	6.5	5.9	5.5	7.2	4.9	4.0
20:4(n-3)	1.1	1.2	1.2	1.4	1.6	0.9	1.6
20:5(n-3)	14.7	20.1	17.9	18.2	18.9	19.7	18.0
22:1(n-11)	7.8	5.4	4.8	4.2	5.7	7.0	4.0
22:6(n-3)	8.9	13.2	13.4	15.5	13.9	11.8	21.6
24:1(n-9)	–	2.3	2.1	2.8	2.3	1.4	2.9
Fatty alcohol							
14:0	5.3	3.3	4.0	6.1	3.4	3.9	2.9
16:0	15.2	14.1	16.5	18.0	17.6	11.9	11.3
16:1(n-7)	9.4	10.6	11.9	9.5	9.9	7.4	6.2
20:1(n-9)	26.8	31.5	30.5	31.2	34.0	31.0	30.8
22:1(n-11)	43.3	33.9	30.2	26.7	30.5	43.6	43.8
Ratios and sums							
ratio 22:1: 20:1	1.6	1.1	1.0	0.9	0.9	1.4	1.4
sum PUFA	36.8	47.2	43.1	45.0	48.7	50.5	54.2
sum MUFA	24.2	26.7	25.8	20.9	27.1	21.8	17.4
sum SAFA	31.6	20.4	29.7	27.3	18.6	22.4	24.2
ratio EPA:DHA	1.7	1.5	1.3	1.2	1.4	1.7	0.8
ratio C16:C18 PUFA	0.6	0.4	0.3	0.3	0.2	0.7	0.3
WE (%total FA + Alc)	54.2	43.1	35.1	15.2	42.9	66.4	32.7

B. Cod larvae

	Station				
Fatty acid	P1	P2	P3	P4	B2
14:0	2.1	3.9	4.7	5.8	2.2
16:0	22.3	14.5	18.2	14.3	23.6
16:1(n-7)	3.7	7.7	6.1	9.1	3.9
16:2(n-4)	–	0.9	–	0.8	–
16:3(n-4)	–	1.6	–	1.8	–
16:4(n-1)	–	2.3	1.9	2.1	–
18:0	10.9	4.4	11.2	2.0	13.9
18:1(n-9)	9.6	4.9	7.0	3.7	8.1
18:1(n-7)	3.1	3.3	2.8	1.6	3.7
18:2(n-6)	–	1.1	2.1	1.5	–
18:4(n-3)	3.1	4.8	4.9	9.5	1.8
20:1(n-9)	4.1	3.3	4.4	6.4	–
20:1(n-7)	–	0.6	–	1.5	–
20:4(n-6)	–	–	–	–	–
20:4(n-3)	–	0.5	–	1.2	–
20:5(n-3)	14.9	18.6	15.1	17.4	13.5
22:1(n-11)	2.7	4.8	5.6	5.7	2.9
22:6(n-3)	23.5	16.5	15.8	10.6	24.8
Fatty alcohol					
14:0	–	5.7	8.7	3.8	–
16:0	–	14.4	14.9	15.1	–
16:1(n-7)	–	8.5	8.9	11.0	–
20:1(n-9)	–	23.2	24.2	31.2	48.1
22:1(n-11)	–	40.6	43.3	28.4	51.9
Ratios and sums					
ratio 22:1: 20:1	–	1.8	1.8	0.9	1.1
sum PUFA	41.5	46.3	39.8	44.9	40.1
sum MUFA	23.2	24.6	25.9	28.0	18.6
sum SAFA	35.3	22.8	34.1	22.1	39.7
ratio EPA:DHA	0.6	1.1	1.0	1.6	0.5
ratio C16:18 PUFA	–	0.8	0.3	0.4	–
WE (%total FA + Alc)	6.5	46.2	43.6	56.4	6.7

of copepods at these locations. This highlights the importance of the extended phytoplankton bloom period in the fjord for continued recruitment success of local and advected *Calanus*. Female *Calanus* at most fjord stations had relatively high amounts of high-energy wax esters and the high levels of 16:1(n7), 20:5(n3), and 22:6(n3) fatty acids suggest that they had been feeding on the phytoplankton spring bloom in April. Cod larvae in Vestfjorden (apart from P1) had high levels of wax esters, indicating that they were feeding on young, non-feeding *Calanus* naupliar stages that still contained wax esters transferred from the mother. *C. finmarchicus* females can transfer wax esters to eggs, which then might prevail in the non-feeding naupliar stages I and II, as has been observed in *C. hyperboreus* (Lee et al., 2006, Jung-Madsen et al., 2013, Leiknes et al., 2016*)*.

On the shelf, our data indicate a temporal mismatch between phytoplankton and *Calanus* during the time of our sampling, however it is likely that a match would be observed a week or so later. The trophic positions calculated for the zooplankton community based on biovolume spectrum theories were extremely low, between trophic level 1 and 2 (1.3 at B2 and 1.5 at B3, respectively). Apparently, the prevailing copepods were not feeding, or had only very recently started to feed. This is consistent with the low $\delta^{15}N$ values derived from older stages of *Calanus* on the shelf. Non-feeding is also indicated by the large difference between $\delta^{13}C$ values of *Calanus* and of POM in this region. Further, *Calanus* females on the shelf (B2 and B3) had low levels of wax esters and a high percentage of the 18:4(n-3) fatty acid, indicative of lipid-poor individuals that had ingested dinoflagellates. Combined, these results point to a recent advection of the older stages onto the shelf, as discussed above (section 4.1.). These results are somewhat conflicting with the observation of the highest chl *a* values and the highest nauplii abundance on the shelf compared to the fjord. However, only older stages were analyzed for stable isotopes (CIV to adults) and fatty acid trophic markers (females). While these stages (G_0) were likely recently advected onto the shelf, the new *Calanus* generation (G_1), which was analyzed for biovolume spectrum theories, was apparently not yet feeding or had just recently started to feed. Cod larvae on the shelf (B2) and at one fjord station (P1) had low levels of wax esters but high levels of the biomembrane fatty acid 22:6(n3), indicating that these larvae did not feed on *Calanus*.

5. Conclusions

We quantified a major inflow of *Calanus*, predominantly *C. finmarchicus*, into Vestfjorden and observed intrusions of Atlantic Water containing high-abundance patches of *Calanus* onto the shelf during our cruise at the end of April. The input of these advected older *Calanus* stages on the lower trophic level shelf food web appeared to be rather limited during our cruise. Essentially, our results suggest two different sources of the *Calanus* population in Vestfjorden and on the shelf: one fraction overwintered locally or in deep fjords nearby and started ascending early to feed on the phytoplankton bloom that peaked around April 11 in Vestfjorden. The other fraction had only recently (end of April) been and still was being advected into the fjord and onto the shelf from the oceanic overwintering habitats.

The fjord food web was tightly coupled between the phytoplankton spring bloom, the local part of the dominating *Calanus* population and the cod larvae. On the shelf, our results suggest that the impact of advected *Calanus* on the food web is at its starting point. Also in the fjord, the advected copepods will ascend in the near future and depending on retention in the fjord, possibly assisted by persistent local eddies, will then contribute to the fjord food web. The prolonged bloom period in Vestfjorden and on the northern Norwegian shelf can ensure a match also with the phenological development of the advected oceanic *Calanus*.

The northern Norwegian fjord-shelf system of the Lofoten and Vesterålen islands supports an economically important fishery on Northeast Arctic cod that has taken place in March-April since the iron age (Bertelsen, 1992, Sundby & Nakken, 2008, (Perdikaris, 1999). Here we have highlighted important factors that can contribute to this: an extended phytoplankton bloom that can support both locally and advected *Calanus*, which in turn can supply the essential nauplii prey for first-feeding cod larvae over several weeks.

CRediT authorship contribution statement

S.L. Basedow: Writing – review & editing, Writing – original draft, Visualization, Validation, Supervision, Software, Methodology, Investigation, Formal analysis, Data curation, Conceptualization. **A. Renner:** Writing – review & editing, Writing – original draft, Visualization, Software, Methodology, Formal analysis, Data curation. **B. Espinasse:** Writing – review & editing, Writing – original draft, Visualization, Supervision, Software, Methodology, Investigation, Formal analysis, Data curation. **S. Falk-Petersen:** Writing – review & editing, Writing – original draft, Validation, Resources, Methodology, Investigation, Conceptualization. **M. Graeve:** Writing – review & editing, Writing – original draft, Validation, Methodology, Formal analysis. **K. Bandara:** Writing – review & editing, Investigation. **K. Sørensen:** Writing – review & editing, Resources, Data curation. **K. Eiane:** Writing – review & editing. **W. Hagen:** Writing – review & editing.

Declaration of competing interest

The authors declare that they have no known competing financial interests or personal relationships that could have appeared to influence the work reported in this paper.

Data availability

Data will be made available on request.

Acknowledgements

We thank captain and crew of R/V “Helmer Hanssen”, as well as the engineers of UiT The Arctic University of Norway for support with instruments and sampling. We thank the LIENS institute for analyses of stable isotopes. The FerryBox data were provide from the Norwegian Ships of Opportunity Program for marine and atmospheric research – NorSOOP (www.norsoop.com) and we thank Dag Øystein Hjermann (NIVA) for the data analysis.

Funding

Field work was carried out as part of the LoVe Marine Ecology project, financed by Equinor, Norway, contract no. 4502610853. Data were analyzed within the Stressor project, financed by the Norwegian Research Council, Norway, as project no. 287043.

Appendix A. Supplementary material

Supplementary data to this article can be found online at https://doi.org/10.1016/j.pocean.2024.103268.

References

Aksnes, D., Aure, J., Kaartvedt, S., Magnesen, T., Richard, J., 1989. Significance of advection for the carrying capacities of fjord populations. Mar. Ecol. Prog. Ser. 50, 263–274.

Albretsen, J., Sperrevik, A. K., Staalstrøm, A., Sandvik, A. D., Vikebø, F., Asplin, L., 2011. NorKystQ 800 report no. 1: User manual and technical descriptions. Fisken og havet 2, Havforskningsintituttets rapportserie, Institute of Marine Research.

Arashkevich, E.G., Tande, K.S., Pasternak, A.F., Ellertsen, B., 2004. Seasonal moulting patterns and the generation cycle of *Calanus finmarchicus* in the NE Norwegian Sea, as inferred from nathobase structures, and the size of gonads and oil sacs. Mar. Biol. 146, 119–132. https://doi.org/10.1007/s00227-004-1416-5.

Bagøien, E., Melle, W., Kaartvedt, S., 2012. Seasonal development of mixed layer depths, nutrients, chlorophyll and *Calanus finmarchicus* in the Norwegian Sea – a basin-scale habitat comparison. Prog. Oceanogr. 103, 58–79. https://doi.org/10.1016/j.pocean.2012.04.014.

Basedow, S.L., Eiane, K., Tverberg, V., Spindler, M., 2004. Advection of zooplankton in an Arctic fjord (Kongsfjorden, Svalbard). Estuar. Coast. Shelf Sci. 60, 113–124. https://doi.org/10.1016/j.ecss.2003.12.004.

Basedow, S.L., Edvardsen, E., Tande, K.S., 2006. Spatial patterns of surface blooms and recruitment dynamics of *Calanus finmarchicus* in the NE Norwegian Sea. J. Plankton Res. 28, 1181–1190. https://doi.org/10.1093/plankt/fbl048.

Basedow, S.L., Tande, K., Zhou, M., 2010. Biovolume spectrum theories applied: spatial patterns of trophic levels within a mesozooplankton community at the polar front. J. Plankton Res. 32, 1105–1119. https://doi.org/10.1093/plankt/fbp110.

Basedow, S.L., Tande, K.S., Norrbin, M.F., Kristiansen, S., 2013. Capturing quantitative zooplankton information in the sea: Performance test of laser optical plankton counter and video plankton recorder in a *Calanus finmarchicus* dominated summer situation. Prog. Oceanogr. 108, 72–80. https://doi.org/10.1016/j.pocean.2012.10.005.

Basedow, S.L., De Silva, N.A.L., Bode, A., Van Beusenkorn, J., 2016. Trophic positions of mesozooplankton across the North Atlantic: estimates derived from biovolume spectrum theories and stable isotope analyses. J. Plankton. Res. 38, 1364–1378. https://doi.org/10.1093/plankt/fbw070.

Basedow, S.L., Sundfjord, A., Von Appen, W.-J., Halvorsen, E., Kwasniewski, S., Reigstad, M., 2018. Seasonal variation in transport of zooplankton into the Arctic Basin through the Atlantic Gateway. Fram Strait. *Front. Mar. Sci.* 5, 194. https://doi.org/10.3389/fmars.2018.00194.

Bertelsen, R. (1992) An archaeological perspective on the medieval north-south connection. In: Medieval Europe 1992 Exchange and Trade Pre-Printed Papers (anonymous), pp. 177-84.

Bøe, R., Bellec, V.K., Dolan, M.F.J., Buhl-Mortensen, P., Buhl-Mortensen, L., Slagstad, D., Rise, L., 2009. Giant sandwaves in the Hola glacial trough off Vesterålen, North Norway. Mar. Geol. 267, 36–54. https://doi.org/10.1016/j.margeo.2009.09.008.

Børve, E., Isachsen, P.E., Nøst, O.A., 2021. Rectified tidal transport in Lofoten-Vesterålen, northern Norway. Ocean Sci. 17, 1753–1773. https://doi.org/10.5194/os-17-1753-2021.

Bustos, C.A., Balbontin, F., Landaeta, M.F., 2007. Spawning of the southern hake Merluccius australis (Pisces: Melucciidae) in Chilean fjords. Fish. Res. 83, 23–32. https://doi.org/10.1016/j.fishres.2006.08.010.

Bustos, C.A., Landaeta, M.F., Balbontin, F., 2008. Spawning and early nursery areas of anchoveta *Engraulis ringens* Jenyns, 1842 in fjords of southern Chile. Revista De Biología Marina y Oceanografía 43, 381–389. https://doi.org/10.4067/S0718-19572008000200014.

Campbell, R.G., Wagner, M.M., Teegarden, G.J., Boudreau, C.A., Durbin, E.G., 2001. Growth and development rates of the copepod *Calanus finmarchcus* reared in the laboratory. Mar. Ecol. Prog. Ser. 221, 161–183. https://doi.org/10.3354/meps221161.

Choquet, M., Hatlebakk, M., Dhanasiri, A.K.S., Kosobokova, K., Smolina, I., Søreide, J., Svensen, C., Melle, W., et al., 2017. Genetics redraws pelagic biogeography of *Calanus*. Biol. Lett. 13 https://doi.org/10.1098/rsbl.20170588.

Coyle, K.O., Gibson, G.A., Hedstrom, K., Hermann, A.J., Hopcroft, R.R., 2013. Zooplankton biomass, advection and production on the northern Gulf of Alaska shelf from simulations and field observations. J. Mar. Sys. 128, 185–207. https://doi.org/10.1016/j.jmarsys.2013.04.018.

Cushing, D.H., 1990. Plankton production and year-class strength in fish populations: an update of the Match/Mismatch hypothesis. Adv. Mar. Biol. 26, 249–293. https://doi.org/10.1016/S0065-2881(08)60202-3.

Degerlund, M., Eilertsen, H.C., 2010. Main species characteristics of phytoplankton spring blooms in the NE Atlantic and Arctic Waters (68–80o N). Estuaries Coast. 33, 242–269. https://doi.org/10.1007/s12237-009-9167-7.

Diel, S., Tande, K.S., 1992. Does the spawning of *Calanus finmarchicus* in high latitudes follow a reproducible pattern? Mar. Biol. 113, 21–31. https://doi.org/10.1007/BF00367634.

Dong, H., Zhou, M., Hu, Z., Zhang, Z., Zhong, Y., Basedow, S.L., Smith, W.O., 2021. Transport barriers and the retention of *Calanus finmarchicus* on the Lofoten shelf in early spring. J. Geophys. Res. Oceans 126: e2021JC017408. https://doi.org/10.1029/2021JC017408.

Dong, H., Zhou, M., Smith, W.O., Li, B., Hu, Z., Basedow, S.L., Gaardsted, F., Zhang, Z., Zhong, Y., 2022. Dynamical controls of the eastward transport of overwintering *Calanus finmarchicus* from the Lofoten Basin to the continental slope. J. Geophys. Res. Oceans 127: e2022JC018909. https://doi.org/10.1029/2022JC018909.

Durant, J.M., Hjermann, D.Ø., Ottersen, G., Stenseth, N.C., 2007. Climate and the match or mismatch between predator requirements and resource availability. Clim. Res. 33, 271–283. https://doi.org/10.2254/cr033271.

Edvardsen, A., Tande, K.S., Slagstad, D., 2003. The importance of advection on production of *Calanus finmarchicus* in the Atlantic part of the Barents Sea. Sarsia 88, 247. https://doi.org/10.1080/00364820310002254.

Edvardsen, A., Pedersen, J.M., Slagstad, D., Semenova, T., Timonin, A., 2006. Distribution of overwintering *Calanus* in the North Norwegian Sea. Ocean Sci. 2, 87–96. https://doi.org/10.5194/os-2-87-2006.

Ellertsen, B., Fossum, P., Solemdal, P., Sundby, S., Tilseth, S. (1987) The effect of biological and physical factors on the survival of Arcto-Norwegian cod and the influence on recruitment variability. Proceedings of the third Sowiet-Norwegian Symposium, Murmansk, 26-28 May 1986.

Espinasse, B., Basedow, S. L., Tverberg, V., Hattermann, T., Eiane, K. (2016b) A major *Calanus finmarchicus* population inside a deep fjord in northern Norway: implications for cod larvae recruitment success. *J. Plankton Res.* 38:604-609, doi:10.1093plankt/fbw024.

Espinasse, B., Tverberg, V., Basedow, S.L., Hattermann, T., Nøst, O.A., Albretsen, J., Skarðhamar, J., Eiane, K., 2016a. Mechanisms regulating inter-annual vaiability in zoopankton advection over the Lofoten shelf, implications for cod larvae survival. Fish. Oceanogr. 26, 299–315. https://doi.org/10.1111/fog.12193.

Falk-Petersen, S., Sargent, J.R., Hopkins, C.C.E., 1990. Trophic relationships in the pelagic arctic food web. In: Barnes, M., Gibson, R.N. (Eds.), Trophic Relationships in the Marine Environment. Scotl. Univ. Press, Aberdeen, pp. 315–333.

Ferreira, A.S.A., Stige, L.C., Neuheimer, A.B., Bogstad, B., Yaragina, N., Prokopchuk, I., Durant, J.M., 2020. Match-mismatch dynamics in the Norwegian-Barents Sea system. Mar. Ecol. Prog. Ser. 650, 81–94. https://doi.org/10.3354/meps13276.

Folch, J., Lees, M., Stanley, G.H.S., 1957. A simple method for the purification of total lipides from animal tissues. J. Biol. Chem. 226, 497–509. https://doi.org/10.1016/S0021-9258(18)64849-5.

Forest, A., Tremblay, J., Gratton, Y., Martin, J., Gagnon, J., Darnis, G., Sampei, M., Fortier, L., et al., 2011. Biogenic carbon flows through the planktonic food web of the Amundsen Gulf (Arctic Ocean): A synthesis of field measurements and inverse modeling analyses. Prog. Oceanogr. 91, 410–436. https://doi.org/10.1016/j.pocean.2011.05.002.

Fortier, L., Ponton, D., Gilbert, M., 1995. The match/mismatch hypothesis and the feeding success of fish larvae in ice-covered southeastern Hudson Bay. Mar. Ecol. Prog. Ser. 120, 11–127.

Furnes, G.K., Sundby, S., 1981. Upwelling and wind induced circulation in Vestfjorden. In: Sætre, R., Mork, M. (Eds.), The Norwegian Coastal Current. University of Bergen, pp. 152–177.

Gaardsted, F., Tande, K.S., Basedow, S.L., 2010. Measuring copepod abundance in deep-water winter habitats in the NE Norwegian Sea: intercomparison of results from laser optical plankton counter and multinet. Fish. Oceanogr. 19, 480–492. https://doi.org/10.1111/j.1365-2419.2010.00558.x.

Gaardsted, F., Tande, K.S., Pedersen, O., 2011. Vertical distribution of overwintering *Calanus finmarchicus* in the NE Norwegian Sea in relation to hydrography. J. Plankton Res. 33, 1477–1486. https://doi.org/10.1093/plankton/fbr042.

Geoffroy, M., Daase, M., Cusa, M., Darnis, G., Graeve, M., Hernandez, N.S., Berge, J., Renaud, P.E., Cottier, F., Falk-Petersen, S., 2019. Mesopelagic sound scattering layers of the high Arctic: seasonal variations in biomass, species assemblage, and trophic relationships. Front. Mar. Sci. 6, 364. https://doi.org/10.3389/fmars.2019.00364.

Giering, S.L.C., Wells, S.R., Mayers, K.M.J., Schuster, H., Cornwell, L., Fileman, E., Atkinson, A., Cook, K.B., Preece, C., Mayor, D.J., 2018. Seasonal variation of zooplankton community structure and trophic position in the Celtic Sea: a stable isotope and biovolume spectrum approach. Prog. Oceanogr. 177, 101943 https://doi.org/10.1016/j.pocean.2018.03.012.

Gillibrand, P.A., Amundrud, T.L., 2007. A numerical study of the tidal circulation and buoyancy effects in a Scottish fjord: Loch Torridon. J. Geophys. Res. Oceans 112. https://doi.org/10.1029/2006JC003806.

Heath, M.R., Boyle, P.R., Gislason, A., Curney, W.S.C., Hay, S.J., Head, E.J.H., Holmes, S., Ingvardsdóttir, A., et al., 2004. Comparative ecology of over-wintering *Calanus finmarchicus* in the northern North Atlantic, and implications for life-cycle patterns. ICES J. Mar. Sci. 61, 698–708. https://doi.org/10.1016/j.icesjms.2004.03.013.

Heath, M.R., Lough, R.G., 2007. A synthesis of large-scale patterns in the planktonic prey of larval and juvenile cod (Gadus morhua). Fish. Oceanogr. 16, 169–185. https://doi.org/10.1111/j.1365-2419.2006.00423.x.

Heneghan, R.F., Everett, J., Blanchard, J.L., Richardson, A.J., 2016. Zooplankton are not fish: improving zooplankton realism in size-spectrum models mediates energy transfer in food webs. Front. Mar. Sci. 3, 201. https://doi.org/10.3389/fmars.2016.00201.

Herman, A.W., Beanlands, B., Chin-Yee, M., Furlong, A., Snow, J., Young, S., Phillips, E. F., 1998. The Moving Vessel Profiler (MVP): in-situ sampling of plankton and physical parameters at 12 knts and integration of a new laser/optical plankton counter. Proc. Oceanol. Int. 102, 123–135.

Herman, A.W., Beanlands, B., Phillips, E.F., 2004. The next generation of Optical Plankton Counter: the Laser-OPC. J. Plankton Res. 26, 1135–1145. https://doi.org/10.1093/plankt/fbh095.

Hjort, J., 1926. Fluctuations in the year classes of important food fishes. ICES J. Mar. Sci. 1, 5–38. https://doi.org/10.1093/icesjms/1.1.5.

Höffle, H., Solemdal, P., Korsbrekke, K., Johannessen, M., Bakkeplass, K., Kjesbu, O.S., 2014. Variability of northeast Arctic cod (Gadus morhua) distribution on the main spawning grounds in relation to biophysical factors. ICES J. Mar. Sci. 71, 1317–1331. https://doi.org/10.1093/icesjms/fsu126.

Hygum, B.H., Rey, C., Hansen, B.W., Carlotti, F., 2000. Rearing cohorts of Calanus finmarchicus (Gunnerus) in mesocosms. ICES J. Mar. Sci. 57, 1740–1751. https://doi.org/10.1006/jmsc.2000.0956.

Jung-Madsen, S., Nielsen, T.G., Grønkjær, P., Hansen, B.W., Møller, E.F., 2013. Early development of *Calanus hyperboreus* nauplii: response to a changing ocean. Limnol. Oceanogr. 50, 2109–2121. https://doi.org/10.4319/lo.2013.58.6.2109.

Kattner, G., Fricke, H.S.G., 1986. Simple gas-liquid chromatographic method for the simultaneous determination of fatty acids and alcohols in wax esters of marine organisms. J. Chromatogr. 361, 263–268. https://doi.org/10.1016/S0021-9673(01)86914-4.

Kattner, G., Krause, M., 1989. Seasonal variations of lipids (wax esters, fatty acids and alcohols) in calanoid copepods from the North Sea. Mar. Chem. 26, 261–275. https://doi.org/10.1016/0304-4203(89)900007-8.

Kitamura, M., Amakasu, K., Kikuchi, T., Nishino, S., 2017. Seasonal dynamics of zooplankton in the southern Chukchi Sea revealed from acoustic backscattering strength. Cont. Shelf. Res. 133, 47–58. https://doi.org/10.1016/j.csr.2016.12.009.
Klungsøyr, J., Tilseth, S., Wilhelmsen, S., Falk-Petersen, S., Sargent, J.R., 1989. Fatty acid composition as an indicator of food intake in cod larvae *Gadus morhua* from Lofoten, Northern Norway. Mar. Biol. 102, 183–188. https://doi.org/10.1007/BF00428278.
Lee, R.E., Hagen, W., Kattner, G., 2006. Lipid storage in marine zooplankton. Mar. Ecol. Prog. Ser. 307, 273–306. https://doi.org/10.3354/meps307273.
Leiknes, Ø., Etter, S.A., Tokle, N.E., Bergvik, M., Vadstein, O., Olsen, Y., 2016. The effect of essential fatty acids for the somate growth in nauplii of *Calanus finmarchicus*. Front. Mar. Sci. 3, 33. https://doi.org/10.3389/fmars.2016.00033.
Meng, R., Smith Jr., W.O., Basedow, S.L., 2023. Spring phytoplankton distributions and primary productivity in waters off northern Norway. J. Mar. Sys. 240, 103891 https://doi.org/10.1016/j.marsys.2023.103891.
Mitchelson-Jacob, G., Sundby, S., 2001. Eddies of Vestfjorden, Norway. Cont. Shelf Res. 21, 1901–1918. https://doi.org/10.1016/S0278-4343(01)00030-9.
Norkko, A., Thrush, S.F., Cummings, V.J., Gibbs, M.M., Andrew, N.L., Norkko, J., Schwarz, A., 2007. Trophic structure of coastal Antarctic food webs associated with changes in sea ice and food supply. Ecol. 88, 2810–2820. https://doi.org/10.1890/06-1396.1.
Ohman, M., Powell, J. R., Picheral, M., Jensen, D. W. (2012) Mesozooplankton and particulate matter responses to a deep-water frontal system in the southern California Current System. *J. Plankton. Res.* 34:815-827, doi:10.1093/plankt/fbs028.
Opdal, A.F., Vikebø, F., 2016. Long-term stability in modelled zooplankton influx could uphold major fish spawning grounds on the Norwegian continental shelf. Can. J. Fish. Aquat. Sci. 73, 189–196. https://doi.org/10.1139/cjfas-2014-0524.
Østerhus, S., Turrell, W. R., Hansen, B., Blindheim, J., van Bennekorn, J. (1996) Changes in the Norwegian Sea Deep Water. *Annual Science Conference 1996, Reykjavik, Iceland. C.M. Document* O:11, doi:10.17895/ices.pub.21286308.
Ottersen, G., Bogstad, B., Yaragina, N.A., Stige, L.C., Vikebø, F., Dalpadado, P., 2014. A review of early life history dynamics of Barents Sea cod (Gadus morhua). ICES J. Mar. Sci. 71, 2064–2087. https://doi.org/10.1093/icesjms/fsu037.
Pedersen, T., 2022. Comparison between trophic positions in the Barents Sea estimated from stable isotope data and a mass balance model. Front. Mar. Sci. 9, 813977 https://doi.org/10.3389/fmars.2022.813977.
Pedersen, O.P., Slagstad, D., Tande, K.S., 2003. Hydrodynamic model forecast as a guide for process studies on plankton and larval fish. Fish. Oceanogr. 12, 369–380. https://doi.org/10.1046/j.1365-2419.2003.00267.x.
Pepin, P., Dower, J.E., 2007. Variability in the trophic position of larval fish in a coastal pelagic ecosystem based on stable isotope analysis. J. Plankton Res. 29, 727–737. https://doi.org/10.1093/plankt/fbm052.
Pepin, P., Orr, D.C., Anderson, J.T., 1997. Time to hatch and larvae size in relation to temperature and egg size in Atlantic cod (Gadus morhua). Can. J. Fish. Aqu. Sci. 54, 2–10. https://doi.org/10.1139/sjfas-54-S1-2.
Perdikaris, S., 1999. From chiefly provisioning to commercial fishery: Long-term economic change in Arctic Norway. World Archaeol. 30, 388–402. https://doi.org/10.1080/00438243.1999.9980419.
Petersen, W., Colijn, F., Elliot, J., Howarth, M. J., Hydes, D. J., Kaitala, S., Kontoyiannis, H., Lavín, A. et al. (2006) European FerryBox project: from online oceanographic measurements to environmental information. In: Dahlin, H. et al. (eds.). European Operational Oceanography: Present and Future. *Proceedings of the 4th EuroGOOS Conference, Brest (France)*, ISBN 92-894-9722-2.
Platt, T., Denman, K., 1978. The structure of pelagic marine ecosystems. Rapp. p.-v. Reun. Cons. Int. Explor. Mer. 173, 60–65.
Sætre, R. (ed) (2007) The Norwegian Coastal Current. Tapir Academic press, 159 pp., ISBN 9788251921848.
Schnack, S.B., 1979. Feeding of *Calanus helgolandicus* on phytoplankton mixtures. Mar. Ecol. Prog. Ser. 1, 41–47.
Seitz, A.C., Michalsen, K., Nielsen, J.L., Evans, M.D., 2014. Evidence of fjord spawning by southern Norwegian Atlantic halibut (Hippoglossus hippoglossus). ICES J. Mar. Sci. 71, 1142–1147. https://doi.org/10.1093/icesjms/fst227.
Silva, E., Counillon, F., Brajard, J., Korosov, A., Pettersson, L.H., Samuelsen, A., Keenlyside, N., 2021. Twenty-one years of phytoplankton bloom phenology in the Barents, Norwegian and North Sea. Front. Mar. Sci. 8, 746327 https://doi.org/10.3389/fmars.2021.746327.
Skjoldal, H.R., Aarflot, J.M., Bagøien, E., Skagseth, Ø., Rønning, J., Lien, V.S., 2021. Seasonal and interannual variability in abundance and population development of Calanus finmarchicus at the western entrance to the Barents Sea, 1995–2019. Prog. Oceanogr. 195, 102574 https://doi.org/10.1016/j.pocean.2021.102574.
Skreslet, S., 1989. Spatial match and mismatch between larvae of cod (Gadus morhua L.) and their principal prey, nauplii of Calanus finmarchicus (Gunnerus). Rapp. P.-V. Réun. Cons. Int. Explor. Mer 191, 258–268.
Skreslet, S., Olsen, K., Mohus, Å., Tande, K.S., 2000. Stage-specific habitats of *Calanus finmarchicus* and *Calanus helgolandicus* in a stratified northern Norwegian fjord. ICES J. Mar. Sci. 57, 1656–1663. https://doi.org/10.1006/jmsc.2000.0968.
Slagstad, D., Tande, K.S., 1996. The importance of seasonal vertical migration in across shelf transport of *Calanus finmarchicus*. Ophelia 44, 189–205. https://doi.org/10.1080/00785326.1995.10429847.
Slagstad, D., Tande, K.S., 2007. Structure and resilience of overwintering habitats of *Calanus finmarchicus* in the Eastern Norwegian Sea. Deep Sea Res. II 54, 2702–2715. https://doi.org/10.1016/j.dsr2.2007.08.024.
Sørensen, K., Durand, D., Folkestad, A., Magnusson, J., Wehde., H. (2008). Operational high-frequency observations from Ferrybox. Proceedings from 5th EuroGOOS Conference, Exeter, UK, May 2008.
Strand, E., Bagøien, E., Edwards, M., Broms, C., Klevjer, T., 2020. Spatial distributions and seasonality of four *Calanus* species in the Northeast Atlantic. Prog. Oceanogr. 185, 102344 https://doi.org/10.1016/j.pocean.2020.102344.
Sundby, S., Nakken, O., 2008. Spatial shifts in spawning habitats of Arcto-Norwegian cod related to multidecadal climate oscillations and climate change. ICES J. Mar. Sci. 65, 953–962. https://doi.org/10.1093/icesjms/fsn085.
Sundby, S. (1978) In/outflow of Coastal Water in Vestfjorden. ICES CM documents C:51.
Trudnowska, E., Stemmann, L., Blachowiak-Samolyk, K., Kwasniewski, S., 2020. Taxonomic and size structure of zooplankton communities in the fjords along the Atlantic water passage to the Arctic. J. Mar. Sys. 204, 103306 https://doi.org/10.1016/j.jmarsys.2020.103306.
Vikebø, F.B., Strand, K.O., Sundby, S., 2019. Wind intensity is key to phytoplankton spring bloom under climate change. Front. Mar. Sci. 6, 518. https://doi.org/10.2289/fmars.2019.00518.
Vikebø, F.B., Broch, O.J., Endo, C.A.K., Frøysa, H.G., Carroll, J., Juselius, J., Langangen, Ø., 2021. Northeast Arctic cod and prey match-mismatch in a high-latitude spring-bloom system. Front. Mar. Sci. 8, 767191 https://doi.org/10.3389/fmars.2021.767191.
Weidberg, N., Basedow, S.L., 2019. Long-term variability in overwintering copepod populations in the Lofoten Basin: the role of the North Atlantic oscillation and trophic effects. Limnol. Oceanogr. 64, 2044–2058. https://doi.org/10.1002/lno.11168.
Willis, K., Cottier, F., Kwasniewski, S., Wold, A., Falk-Petersen, S., 2006. The influence of advection on zooplankton community composition in an Arctic fjord (Kongsfjorden, Svalbard). J. Mar. Sys. 61, 39–54. https://doi.org/10.1016/j.jmarsys.2005.11.013.
Zhou, M., 2006. What determines the slope of a plankton biomass spectrum? J. Plankton Res. 28, 437–448. https://doi.org/10.1093/plankt/fbi119.
Zhou, M., Huntley, M., 1997. Population dynamics theory of plankton based on biomass spectra. Mar. Ecol. Prog. Ser. 159, 61–73.